Supramolecular Aggregates of Azobenzene Phospholipids and Related Compounds in Bilayer Assemblies and Other Microheterogeneous Media: Structure, Properties, and Photoreactivity[1]

Xuedong Song, Jerry Perlstein, and David G. Whitten*

Contribution from the Department of Chemistry and NSF Center for Photoinduced Charge Transfer, University of Rochester, Rochester, New York 14627

Received April 23, 1997[⊗]

Abstract: A number of phosphatidyl choline derivatives containing *trans*-azobenzene units in the fatty ester backbone have been synthesized and studied in aqueous dispersions both pure and in the presence of saturated and unsaturated phospholipids. The structures of the assemblies formed have been investigated by microcalorimetry, dynamic light scattering, cryo-transmission electron microscopy, and reagent entrapment. While many of the mixed phospholipid dispersions give evidence for the formation of small unilamellar vesicles, the aqueous dispersions of pure azobenzene phospholipids (APL's) give evidence for several different structures, including relatively large plates in at least one case. The azobenzenes show strong evidence of "H" aggregate formation both in the pure and mixed dispersions. The aggregation number has been estimated for several of the APL's and found to be typically 3 or a multiple thereof. On the basis of simulations and studies with similar stilbene phospholipids as well as on the strong induced circular dichroism signals observed for the aggregate, we infer a chiral "pinwheel" unit aggregate structure similar to that found for several aromatics. The azobenzenes in the aqueous dispersions have been found to photoisomerize to give *cis*-rich photostationary states; the *cis*-azobenzenes show no evidence for aggregation and no induced circular dichroism. The *cis*-azobenzenes can be isomerized back to the *trans* either by irradiation or by thermal paths. Mixed aqueous dispersions of *trans*-APL's with saturated or unsaturated phospholipids can be prepared which entrap the fluorescent dye carboxyfluorescein (CF) under conditions where the CF fluorescence is very low due to self-quenching. By varying the APL/host phospholipid ratio the azobenzene can be aggregate, monomer, or dimer. In cases where the azobenzene is monomer or dimer, irradiation produces complete isomerization but little "leakage" of CF from the vesicle interior. In contrast, where the azobenzene is predominantly aggregate, irradiation results in both photoisomerization and reagent release. That photoisomerization in the latter case can result in "catastrophic" destruction of the vesicle can also be shown by cryo-transmission electron microscopy.

Introduction

The thermal and photoisomerization reactions of azobenzenes have been found to occur in a wide variety of media in a process formally analogous to the much more widely studied (from a mechanistic perspective) photoisomerization of the stilbenes and related olefins.[2−5] In contrast to the stilbenes, whose photoisomerization shows a high medium sensitivity, azobenzene photoisomerization has been found to occur even in very viscous solutions, liquid crystals, and rigid solids.[6−16] This has led to the use of azobenzene derivatives as a photoresponsive "trigger" for control of macroscopic properties such as volume,[6] wettability,[11] membrane permeability,[12] solubility and viscosity in a number of applications. The most likely explanation for the differences between azobenzene and stilbene photoisomerization is the occurrence of an "inversion" mechanism[4,5] in the case of the azobenzenes which is not available for the stilbenes and alkenes.

In recent investigations we and others have found that amphiphilic stilbene[17] and azobenzene derivatives[18] as well as a number of other functionalized amphiphilies[19,20] containing an aromatic or dye chromophore tend to form relatively stable aggregates when dispersed in aqueous media or incorporated

[⊗] Abstract published in *Advance ACS Abstracts,* September 15, 1997.

(1) A portion of this research has appeared as a communication: Song, X.; Perlstein, J.; Whitten, D. G. *J. Am. Chem. Soc*. **1995**, *117*, 7816.
(2) Saltiel, J.; Charlton, J. L. In *Rearrangements in Ground and Excited State*; de Mayo, P., Ed.; Academic Press, New York, 1980; Vol. 3.
(3) Siapiringue, N.; Guyot, G.; Monti, S.; Bortulis, P. *J. Photochem.* **1987**, *37*, 185.
(4) Hammond, G.; Saltiel, J.; Lamola, A. A.; Turro, N. J.; Bradashaw, G. S.; Cowan, D. O.; Counsell, R. S.; Vogt, V.; Dalton, C. *J. Am. Chem. Soc.* **1964**, *86*, 3197.
(5) Jones, L. B.; Hammond, G. *J. Am. Chem. Soc*. **1965**, *87*, 4219.
(6) (a) Rau, H.; Liiddecke, E. *J. Am. Chem. Soc.* **1982**, *104*, 1616. (b) Rau, *J. Photochem*. **1984**, *26*, 21.
(7) Monti, S.; Orlandi, G.; Palmieri, P. *Chem. Phys*. **1982**, *71*, 87.
(8) Eisenbach, C. D. *Ber. Bunsen-Ges. Phys. Chem*. **1980**, *84*, 680.
(9) Yamamoto, A. *Macromolecules* **1986**, *19*, 2472.
(10) Lamarre, L.; Sung, C. S. P. *Macromolecules* **1983**, *16*, 1729.
(11) (a) Ishihara, K.; Namada, N.; Kato, S.; Shinohara, I. *J. Polym. Sci., Polym. Chem. Ed*. **1984**, *22*, 121. (b) Ishihara, K.; Namada, N.; Kato, S.; Shinohara, I. *J. Polym. Sci., Polym. Chem. Ed*. **1983**, *21*, 1551.
(12) Okahata, Y.; Fujita, S.; Iizuka, N. *Angew. Chem., Intl. Ed. Engl*. **1986**, *25*, 751.
(13) Bortolus, P.; Monti, S. *J. Phys. Chem*. **1987**, *91*, 5046.
(14) Shinkai, S.; Matsuo, K.; Harada, A.; Manabe, O. *J. Chem. Soc., Perkin Trans. II* **1982**, 1261.
(15) Hentze, F. *Z. Chem*. **1977**, *17*, 294.
(16) Haberfield, P. *J. Am. Chem. Soc*. **1987**, *109*, 6177.
(17) (a) Whitten, D. G. *Acc. Chem. Res.* **1993**, *26*, 502. (b) Song, X.; Geiger, C.; Furman, I.; Whitten, D. G. *J. Am. Chem. Soc*. **1994**, *116*, 4103. (c) Song, X.; Geiger, C.; Leinhos, U.; Perlstein, J.; Whitten, D. G. *J. Am. Chem. Soc*. **1994**, *116*, 10340.
(18) (a) Heesemann, J. *J. Am. Chem. Soc.* **1980,** 102, 2167. (b) Fukuda, K.; Nakahara, H. *J. Colloid Interface Sci*. **1980**, 98, 555. (c) Kunitake, T. *Angew. Chem., Int. Ed. Engl*. **1992**, *31*, 709.
(19) (a) Chen, H.; Farahat, M.; Law, K. Y.; Perlstein, J.; Whitten, D. G. *J. Am. Chem. Soc*. **1996**, *118*, 2586. (b) Chen, H.; Law, K. Y.; Perlstein, J.; Whitten, D. G. *J. Am. Chem. Soc*. **1995**, *117*, 7257.
(20) Farahat, C. W.; Penner, T. L.; Ulman, A.; Whitten, D. G. *J. Phys. Chem*. **1996**, *100*, 12616

S0002-7863(97)01291-2 CCC: $14.00

into monolayer films at the air−water interface. Although it was initially thought that these aggregates were formed as a consequence of self-organization of the functionalized amphiphiles into a relatively ordered structure, more extensive investigations have shown that the aggregates are stabilized by strong noncovalent aromatic−aromatic interactions and tend to form readily in the presence of water, even before major amphiphile organization has occurred.[21] For several aromatics and dyes the key species in forming these aggregates is a "unit aggregate" which is in many cases a trimer or tetramer, which has been proposed to be a chiral "pinwheel" structure based both on simulations and experimental evidence.[1,17,21] Our studies suggest that the extended aggregates in several assemblies are probably best described as a mosaic or lattice of the small "unit" aggregates. Aggregation has been found especially prominent when the functionalized amphiphiles are incorporated into phospholipid bilayers, either as "guests" solubilized within the bilayer generated by a "host" phospholipid or when modified phospholipids containing the chromophore are themselves dispersed in aqueous media. Since saturated phospholipids and structurally related amphiphiles form small unilamellar closed spherical vesicles upon dispersion and probe sonication in aqueous solution which can entrap reagents, a number of investigations[22−24] have sought to prepare vesicles containing a photoreactive component which can be used to promote a controlled release of entrapped reagents in various applications including drug delivery.

In the present paper we report a study of the assemblies formed from several synthetic azobenzene derivatized phospholipids (APL's) in aqueous media, their structures, physical properties, and photochemical behavior. Results of the study of these compounds provide some insights into the importance of aggregation in controlling both the microstructure as well as the macroscopic properties of the assemblies. Some of the key findings include the observation that the *trans*-APL's do not form closed spherical bilayer vesicles upon dispersion in water but rather form a variety of different structures, including large plates or sheets in some cases, presumably due to resistance to cuvature in the extended bilayer. We find that closed vesicles capable of entrapping reagents can be formed when mixtures of *trans*-APL's are codispersed with saturated and unsaturated phospholipids and that, depending upon the state of the incorporated azobenzene as well as the host, controlled release of entrapped reagents may be promoted by photolysis.

Experimental Section

Materials and General Techniques. Synthetic reagents were purchased from Aldrich Chemical Company and used as received unless otherwise stated. Cholesterol (99%); α-, *β*-, and *γ*-cyclodextrins (99+%); and Triton-X-100 were purchased from Aldrich. Rattlesnake venom, L-α-glycero-3-phosphorylcholine as the cadmium chloride complex, Sephedex-50G, L-α-dimyristoylphosphatidylcholine (DMPC, 99+%), D- and L-α-dipalmitoylphosphatidylcholine (DPPC, 99%), and 1-palmitoyl-2-oleoyl-*sn*-glycero-3-phosphocholine (POPC) were obtained from Sigma. All solvents for spectroscopic studies were spectroscopic grade from Fisher or Aldrich. Milli-Q water was obtained by passing in-house distilled water through a Millipore -RO/UF water purification system. Deuterated solvents were purchased from MSD Isotopes or Cambridge Isotope Laboratories. 5(6)-Carboxyfluorescein (CF) was obtained from Eastman Chemical.

Melting points were taken on an El-Temp II melting point apparatus and are uncorrected. The pH values were measured with an Orien Research digital ionalyzer/501 pH meter. Proton NMR spectra were recorded on a General Electric QE300 MHz spectrometer using deuterated solvent locks or on a 500 MHz Varian VXR-500S spectrometer. FAB mass spectra were measured at the Midwest Center for Mass Spectrometry. Absorption spectra were obtained on a Hewlett-Packard 8452A diode array spectrophotometer. Fluorescence spectra were recorded on a SPEX Fluorolog-2 spectrofluorometer and were not corrected. The circular dichroism (CD) study was carried out on a JASCO J-710 spectropolarimeter. Differential scanning calorimetry (DSC) measurements were carried out on a Mc-2 Ultrasensitive Scanning Calorimeter from MicroCal, Inc. Size extrusion experiments for vesicles were performed with an extruder through CoStar Nucleopore Polycarbonate Filters. Dynamic light-scattering measurements were carried out at the Eastman Kodak Research Laboratories.[25] All samples were routinely filtered through a 1.2 μm nylon syringe filter before data acquisition. Cryo-transmission electron microscope measurements (Cryo-TEM) were made either at the Eastman Kodak Research Laboratories[26] or at the laboratory of NSF Center for Interfacial Engineering, Department of Chemical Engineering, University of Minnesota.[26] A 200 W Mercury lamp (Oriel) was used for irradiation. The 365 nm line was separated through an interference filter (365 BP 10, T = 217). An Oriel tungsten lamp (Model 6130) was used to produce intense visible light.

The general methods used for preparing Langmuir−Blodgett films and self-assemblies are based on techniques described by Kuhn et al.[27] Monolayers of chromophore-derivatized fatty acids or phospholipids were prepared by spreading a chloroform solution of material to be studied onto an aqueous surface containing cadmium chloride (2.5×10^{-4} M) and sodium bicarbonate (3×10^{-5} M, pH = 6.6−6.8) on a KSV 5000 automatic film balance at room temperature (23 °C). The monolayers were then transferred onto quartz substrates. Reflectance spectra for monolayers at the air−water interface were recorded with a SD1000 fiber optics spectrometer (Ocean Optics, Inc.) equipped with optical fibers, an LS-1 minature tungsten halogen lamp and a CCD detector.

Bilayer vesicles were prepared according to established protocols.[28] A Cell Disrupter W220F from Heat Systems Ultrasonics, Inc. (setting 6.5, 35 W) was used for probe sonication. The vesicles trapping CF were prepared as following:[29] Depending on the specific vesicle systems, an appropriate amount of DPPC or POPC, and/or APL stock solution and/or cholesterol was dissolved in a small amount of $CHCl_3$. The $CHCl_3$ was removed by a nitrogen stream to form a thin film on the wall of vial, which was then dried under vacuum overnight. An appropriate amount (usually 1−3 mL) of 0.1 M CF aqueous solution (pH = 7.0) was added to the vial and the sample was incubated in a water bath at 65 °C for 20 min. The mixture was vortexed for 20 min followed by a 10−15 min sonication until a clear, transparent solution was obtained. To remove nonentrapped CF, the resulted vesicles were purified via gel filtration on a Sephedex G-50 column, using Milli-Q water as the eluent. The vesicle fraction was collected and stored at 4 °C for DPPC vesicles and at room temperature for POPC vesicles.

The vesicles containing CF from gel filtration were diluted with water to a specific concentration by monitoring the absorption spectra of the samples. Release of CF was monitored by scanning spectrofluorometer at 518 nm with excitation at 492 nm. The irradiation of the sample in a quartz cuvette was made with a mercury lamp with a 365 nm filter. Once the irradiation was complete, the sample was transferred quickly

(21) Chen, H.; Liang, K.; Song, X.; Samha, H.; Law, K. Y.; Perlstein, J.; Whitten, D. G. In *Micelles, Microemulsions and Monolayers: Science and Technology*; Shah, D., Ed.; Marcel Dekker, Inc: New York, 1995; in press

(22) Pidgeon, C.; Hunt, C. A. *Photochem. Photobiol.* **1983**, *37*, 491.

(23) Morgan, C. G.; Thomas, E. W.; Sanhdu, S. S.; Yianni, Y. P.; Mitchell, A. C. *Biochim. Biophys. Acta* **1987**, 504.

(24) Kano, K.; Tanaka, Y.; Ogawa, T.; Shimomura, M.; Kunitake, T. *Photochem. Photobiol.* **1981**, *34*, 323.

(25) The authors thank Dr. Thomas Whitesides at the Eastman Kodak Research Laboratories for light scattering measurements.

(26) The authors thank Dr. John Minter at the Eastman Kodak Research Laboratories and Dr. Michael Bench in the Department of Chemical Engineering, University of Minnesota, for the help with Cryo-TEM studies.

(27) Kuhn, H.; Möbius, D.; Bücher, H. In *Physical Methods of Chemistry*; Weissberger, A., Rossiter, B. W., Eds.; Wiley: New York, 1972; Vol. 1, P577.

(28) (a) Hope, M. J.; Bally, M. B.; Webb, G.; Cullis, P. R. *Biophys. Acta* **1985**, *55*, 812. (b) Saunders, L.; Perrin, J.; Gammock, D. B. *J. Pharm. Pharmacol.* **1962**, *14*, 567.

(29) (a) Weinstein, J. N.; Yoshikami, S.; Henkart, P.; Blumenthal, R.; Hagins, W. A. *Science* **1977**, *195*, 489. (b) Liu, Y.; Regen, S. L. *J. Am. Chem. Soc.* **1993**, *115*, 708. (c) Nagawa, Y.; Regen, S. L. *J. Am. Chem. Soc.* **1992**, *114*, 1668.

to the spectrofluorometer and the fluorescence intensity of CF as a function of time was measured.

Aggregate Size Measurements. A series of samples containing different concentration of APL and the same concentration of DMPC (total volume of each sample was the same) was incubated in a water bath with temperature at or above the T_c for APL vesicles overnight to make sure that the samples were equilibrated. Another pure DMPC sample of the same concentration without APL's was also incubated in the same water bath as a reference for absorption spectra. The ratio of [DMPC]/[APL], which should be larger than 5 to meet the requirement of DMPC as a medium, must be carefully selected so that the equilibrated solutions contain significant concentration of both aggregate and dimer to reduce the experimental error. The samples were transferred as quickly as possible into a warm cuvette in a holder maintained at constant temperature by the same water bath. Absorption spectra were recorded immediately. The absorbance contributions of both aggregates and dimers in equilibrated solutions were obtained by simple spectral subtraction based on the reasonable assumption that the pure APL vesicles have only aggregates and those with APL's highly diluted in DMPC ([DMPC]/[APL] larger than 80) contain only dimer. The plot according to eq 6 allows determination of aggregate sizes.

Sample Preparation for Cryo-Transmission Electron Microscopy (Cryo-TEM). The samples for Cyro-TEM were prepared in dim red light to avoid possible photoisomerization. The vesicles were put into a controlled environment vitrification system unit where the temperature was controlled at just above room temperature and the humidity was nearly 100%. A screened grid was spotted with the sample and blotted slightly to form a thin layer of liquid containing the vesicle particles. The grid was then plunged into liquid ethane to vitrify the liquid and immobilize the vesicles. The sample was transferred under liquid nitrogen to a Cryo-TEM specimen holder where the sample was inserted into the TEM. The sample was held at a temperature of −172 °C. Low dose electron images were taken of various areas of the grid where there were thin layers of vitrified liquid across the holes in the grid.

Synthesis of Azobenzene Derivatives. The structures and acronyms of the compounds used in this study are shown in Chart 1. Synthesis of A_4H and $_4A_4H$ is identical to the reported procedures.[30] The general synthetic scheme for APL's is shown in Scheme 1.

$_4A_4$EPC. The following method is similar to other procedures previously reported.[30,31] Dry $_4A_4H$ (370 mg) was dissolved in 20 mL of dry methylene chloride. Triethylamine (0.4 mL) was added via syringe followed by trimethylacetyl chloride (1.2 mL) under a nitrogen stream. The reaction mixture was stirred for approximately 20 h. The reaction was monitored by TLC (solvent B: $CHCl_3$/methanol/water = 65/25/4). After the reaction was complete, the solvent was removed by rotary evaporation and the residue was dried under vacuum in a dessicator for about 10 h to remove traces of unreacted chloride and triethylamine.

The crude mixed anhydride obtained above was dissolved in 10 mL of dry methylene chloride and added via syringe to a suspension of L-α-glycero-3-phosphorylcholine as the cadmium chloride complex (GPC·$CdCl_2$) (160 mg) and 4-(*N*,*N*-dimethylamino)pyridine (DMAP) (90 mg) in CH_2Cl_2 (4 mL). The mixture was stirred under nitrogen for about 24 h. TLC (solvent B) showed the completion of reaction with only a trace of monosubstituted product. The solvent was removed by rotary evaporation, and the residue was dissolved in solvent B. The solution was passed through an ion exchange column, Rexyn-I 300 to remove the $CdCl_2$ and DMAP. The solvent was removed by rotary evaporation. The crude product was purified by passing it through a Sephedex LH-20 column eluting with chloroform/methanol (50/50) followed by precipitation in ether three times. A total of 140 mg of a dry white powder was obtained. Yield: 44%. ^{1}H NMR (500 MHz, $CDCl_3$), δ: 7.81 (d, J = 7.5, 8 H), 7.30 (d, J = 8.0, 8H), 5.25 (m, 1 H), 4.42 (d, J = 11.5, 1 H), 4.33 (m, 2 H), 4.17 (dd, J = 9,5, 7.0, 1 H), 4.02 (m, 2 H), 3.80 (m, 2 H), 3.31 (s, 9 H), 2.68 (t, J = 7.5, 8 H), 2.34 (q, J = 8.0, 4 H), 1.95 (m, 4 H), 1.64 (5, J = 7.5, 4 H), 1.39 (5, J = 7.0, 4 H), 0.94 (t, J = 7.5, 6 H). FAB: *m*/*z* calcd for $[M + 1]^+$ = 870.4, found 870.4.

(30) Sandhu, S. S.; Yianni, Y. P.; Morgan, C. G.; Taiyor, D. M.; Zaba, B. *Biochim. Biophys. Acta* **1986**, *860*, 253.

(31) Furman, I.; Geiger, C. H.; Whitten, D. G.; Penner, T. L.; Ulman, A. *Langmuir* **1994**, *10*, 837.

Chart 1

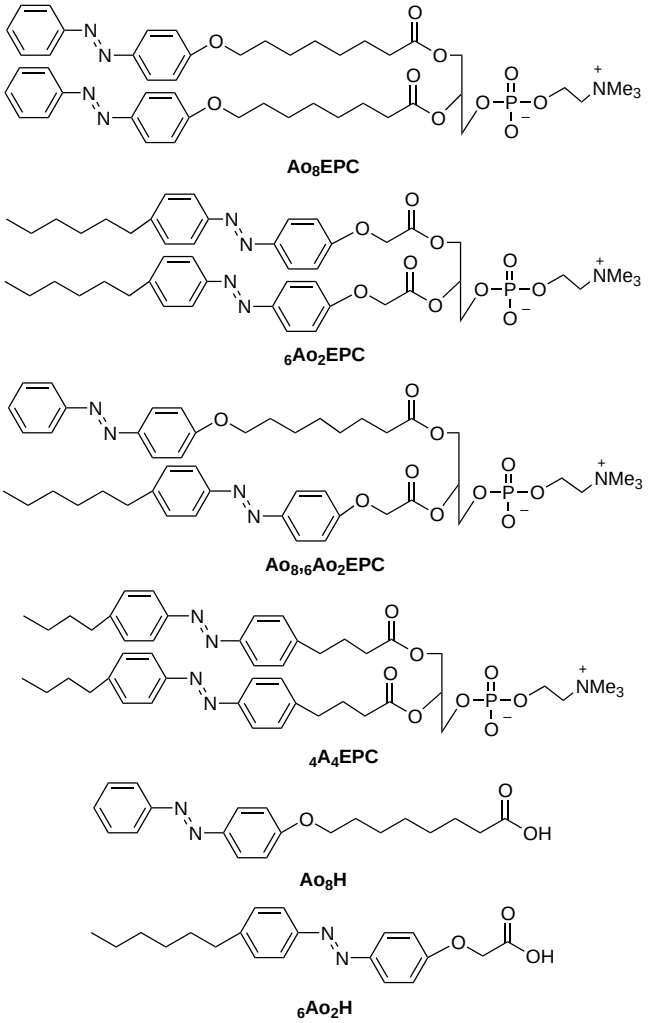

A_4EPC. The preparation procedure is identical to that for $_4A_4$EPC. Yield: 67%. ^{1}H NMR (500 MHz, $CDCl_3$), δ: 7.83 (d, J = 8.1, 4 H), 7.87 (d, J = 8.1, 4 H), 7.50 (m, 6 H), 7.36 (m, 4 H), 5.52 (m, 1 H), 4.40 (m, 3 H), 4.2 (m, 1 H), 4.05 (m, 2 H), 3.85 (s, 9 H), 2.70 (t, J = 7.0, 4 H), 2.40 (t, J = 7.1, 4 H), 1.97 (m, 4 H). FAB: *m*/*z* calcd for $[M + 1]^+$=756.3, found 756.3.

$_6$AoH: *p*-Hexylaniline (7 g) was dissolved in 1:1 aqueous acetone (100 mL), and concentrated HCl (10 mL) was added. The mixture was cooled in an ice bath, and sodium nitrite (2.9 g) dissolved in 50 mL of cold water was added with stirring. After addition, the solution was allowed to stand for 15 min in an ice bath. The diazonium salt solution obtained was slowly added to a cold aqueous solution (100 mL) of phenol (4 g), sodium hydroxide (1.7 g), and sodium carbonate (7 g). The yellow precipitate which appeared was filtered out and recrystallized from a mixed solvent of benzene and hexane. A total of 5.46 g of product was obtained. Yield: 48%. mp: 81−82 °C. ^{1}H NMR (300 MHz, $CDCl_3$), δ: 7.92 (d, 2 H), 7.84 (d, 2 H), 7.30 (d, 2 H), 6.98 (d, 2 H), 2.70 (t, 2 H), 1.70 (m, 2 H), 1.38 (m, 6 H), 0.97 (t, 3 H).

Ao_8H: AoH (3.2 g), $Br(CH_2)_7COOH$ (3.3 g), and potassium hydroxide (1.8 g) were added to a 200 mL round-bottomed flask with ethanol (60 mL). The mixture was refluxed overnight. An orange precipitate was collected by filtration and recrystallized from CH_2Cl_2. A total of 1.5 g of orange crystals was obtained. Yield: 67%. mp: 150−151 °C. ^{1}H NMR (300 MHz, $CDCl_3$), δ: 7.90 (q, J = 9.5, 4 H), 7.50 (m, 3 H), 7.04 (d, J = 9.4, 2 H), 4.06 (t, J = 7.1, 2 H), 2.40 (t, J = 7.1, 2 H), 1.85 (m, 2 H), 1.50 (m, 2 H), 1.25 (m, 4 H).

$_6Ao_2$H: $_6$AoH (3 g), ethyl bromoacetate (1.5 mL), and potassium hydroxide (600 mg) was added to a round-bottomed flask containing 50 mL of ethanol. The mixture was refluxed for 2 h and cooled in an ice bath. A precipitate formed and was collected and recrystalized from pentane. A total of 1.9 g of yellow crystals ($_6Ao_2$M) was obtained.

Scheme 1

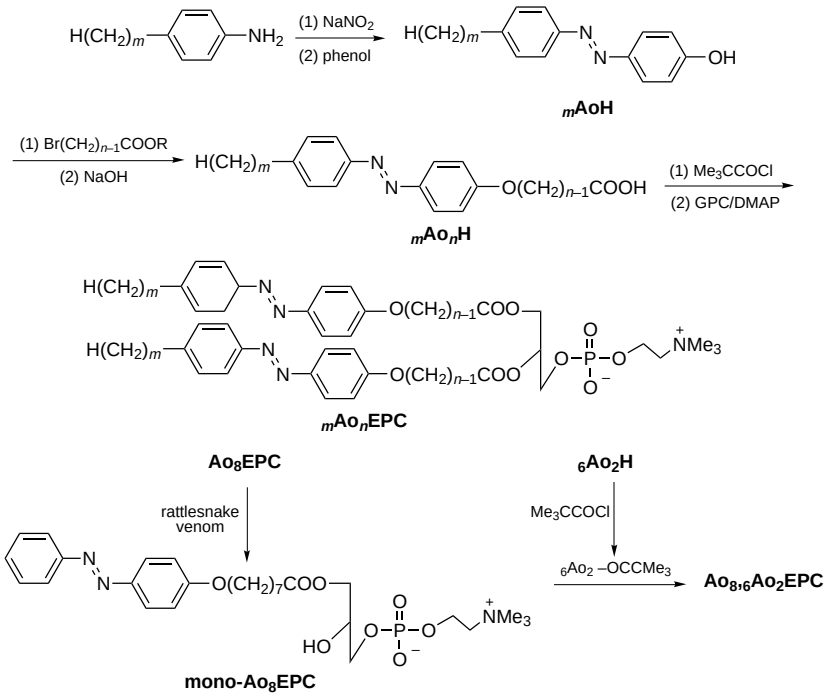

Yield: 52%. ^{1}H NMR (300 MHz, $CDCl_3$), δ: 7.95 (d, $J = 9.6$, 2 H), 7.84 (d, $J = 9.6$, 2 H), 7.34 (d, $J = 9.4$, 2 H), 7.03 (d, $J = 9.4$, 2 H), 4.74 (s, 2 H), 4.32 (q, $J = 5.4$, 2 H), 2.70 (t, $J = 8.3$, 2 H), 1.68 (t, $J = 6.0$, 2 H), 1.32 (m, 8 H), 0.95 (m, 3 H).

$_6$Ao$_2$M (1.8 g) was dissolved in 30 mL of water/methanol (10/90) and to the solution was added sodium hydroxide pellets (800 mg). The mixture was heated to reflux for 15 min and a yellow solid formed. The solid was collected and recrystallized from chloroform containing 2% glacial acetic acid. A total of 1.5 g of a yellow powder was obtained. Yield: 87%. Mp: >260 °C, with decomposition. ^{1}H NMR (300 MHz, DMSO-d_6), δ: 7.95 (d, $J = 9.6$, 2 H), 7.84 (d, $J = 9.6$, 2 H), 7.34 (d, $J = 9.4$, 2 H), 7.03 (d, $J = 9.4$, 2 H), 4.60 (s, 2 H), 2.64 (t, $J = 8.4$, 2 H), 1.60 (m, 2 H), 1.30 (m, 8 H), 0.85 (m, 3 H).

$_6$Ao$_2$EPC: The synthesis is similar to that of $_4$A$_4$EPC. Yield: 54%. ^{1}H NMR (500 MHz, DMSO-d_6), δ: 7.85 (t, $J = 9.3$, 4 H), 7.73 (q, $J = 5.2$, 4 H), 7.33 (m, 4 H), 7.12 (t, $J = 9.3$, 4 H), 5.24 (m, 1 H), 5.90 (m, 4 H), 4.45 (d, $J = 10.3$, 1 H), 4.33 (m, 1 H), 4.07 (m, 2 H), 3.87 (m, 2 H), 3.50 (m, 2 H), 3.12 (s, 9 H), 2.62 (m, 4 H), 2.50 (m, 4 H), 1.57 (m, 4 H), 1.28 (m, 8 H), 0.85 (t, 6 H). FAB: *m*/*z* calcd for $[M + H]^+$ 902.4, found 902.4.

Ao$_8$EPC: The synthesis is similar to that of $_4$A$_4$EPC. Yield: 67%. ^{1}H NMR (500 MHz, $CDCl_3$), δ: 7.89 (q, $J = 8.5$, 8 H), 7.50 (t, $J = 7.5$, 4 H), 7.43 (t, $J = 7.0$, 2 H), 6.99 (d, $J = 7.5$, 4 H), 5.24 (m, 1 H), 4.40 (m, 3 H), 4.15 (dd, $J = 7.0$, 9.5, 1 H), 4.02 (m, 6 H), 3.91 (m, 2 H), 3.39 (s, 9 H), 2.33 (m, 4 H), 1.80 (m, 4 H), 1.63 (m, 4 H), 1.47 (m, 4 H), 1.37 (m, 8 H). FAB: *m*/*z* calcd for $[M + H]^+$ 902.4, found 902.4.

Ao$_8$, $_6$Ao$_2$EPC: A$_8$EPC was dissolved in 3 mL of CH_2Cl_2/methanol (99/1, v/v) followed by addition of an aqueous solution containing 20 mM tris-HCl, pH 8.0, and 40 mM $CaCl_2$, and 2 mg of rattlesnake venom (*Crotalus adamanteous*) was added. The reaction vessel was sealed, and the solution was vortexed for 3 d in the dark. When the reaction was completed, the organic solvent was removed by a stream of nitrogen and the lyso product was extracted by the Bligh−Dyer procedure.[32] Some distilled water was added to the aqueous solution to a total volume of 8 mL followed by addition of 10 mL of $CHCl_3$ and 20 mL of methanol to obtain a clear one-phase solution. Then to the clear mixture was added 10 mL of water and 10 mL of $CHCl_3$ to get a biphasic mixture. The $CHCl_3$ layer was separated, and 20 mL of $CHCl_3$ was added to the methanol−water phase in an additional extraction. The $CHCl_3$ layers were combined, and the solvent was removed by evaporation. Most of the Ao$_8$H byproduct was removed by repeating the precipitation in the mixed solvent of ether and $CHCl_3$. A total of 90 mg of mono-Ao$_8$EPC product was obtained.

The mixed anhydride obtained from the reaction between $_6$Ao$_2$H (130 mg) and trimethylacetyl chloride (0.3 mL) was dissolved in dry methylene chloride and added via a syringe to a suspension of mono-Ao$_8$EPC (45 mg) and 4-(*N*,*N*-dimethylamino)pyridine (DMAP) in 4 mL of CH_2Cl_2. The mixture was sealed and stirred in the dark under nitrogen for about 48 h. TLC (solvent B) indicated the completion of the reaction. The solvent was removed by rotary evaporation and the residue was dissolved in solvent B. The crude product was purified by chromotography (chromatotron) eluting with solvent B. A total of 24 mg of pure product was obtained. Yield: 33%. ^{1}H NMR (500 MHz, $CDCl_3$), δ 7.88 (m, 6 H), 7.78 (d, $J = 7.5$, 2 H), 7.49 (t, $J = 7.6$, 2 H), 7.43 (t, $J = 7.5$, 1 H), 7.28 (d, $J = 9.0$, 2 H), 6.96 (d, $J = 9.0$, 2 H), 5.4 (m, 1 H), 4.84 (d, $J = 16.0$, 1 H), 4.73 (d, $J = 16.0$, 1 H), 4.42 (d, $J = 14$, 1 H), 4.32 (m, 2 H), 4.16 (m, 1 H), 4.08 (m, 2 H), 3.97 (t, $J = 7.1$, 2 H), 3.76 (m, 2 H), 3.27 (s, 9 H), 2.64 (t, $J = 8.0$, 2 H), 2.27 (t, $J = 8.0$, 2 H), 1.80 (m, 2 H), 1.60 (m, 2 H), 1.32 (m, 4 H), 0.88 (t, 3 H). FAB: *m*/*z* calcd for $[M + H]^+$ 902.4, found: 902.4.

Results and Discussion

The structures of the azobenzene (*trans* form unless otherwise stated) amphiphiles synthesized and used in these investigations are shown in Chart 1 together with their acronyms. All of these compounds exhibit good solubility in organic solvents such as chloroform and methylene chloride to give solutions characterized by the typical azobenzene monomer absorption spectra with a weak n−π* transition near 450 nm, an intense π−π* transition (A band) at 348 nm, and a second π−π* transition (B band) at 248 nm (with exception of $_6$Ao$_2$EPC in chloroform, a little broader and 4 nm blue-shifted absorption spectrum relative to the other APL's is observed and assigned to an oblique dimer). In no case have we been able to detect any fluorescence from these compounds either in organic solvents or in other media (see below). The phospholipid derivatives (APL's) shown in Chart 1 can be dispersed by sonication in water, giving clear solutions which, however, obviously scatter light. The short-chain APL, A$_4$EPC, gives an absorption spectrum in water very similar to those obtained for all of the azobenzene amphiphiles in chloroform, suggesting that the chromophore is monomeric. In contrast, all of the other APL's exhibit absorption spectra in the aqueous dispersions characterized by a blue-shifted A band

(32) Bligh, E. G.; Dyer, W. J. *Can. J. Biochem. Physiol*. **1959**, 37, 911.

Table 1. Absorption Spectral Data of APL's in Different Media

	λ_{max}, nm (ϵ)[b]						
	chloroform	water	DMPC	shift,[c] nm	FWHM,[a] nm	B[d]	H[e]
Ao_8EPC	348 (3.6)	317 (3.8)	348 (5.4)	31	41	2.436	0.5659
$_6Ao_2EPC$	344 (4.3)	320 (3.4)	348 (5.2)	28	57	1.765	0.5513
$Ao_{8,6}Ao_2EPC$	348 (3.8)	320 (4.3)	348 (5.3)	28	59	1.653	0.5257
$_4A_4EPC$	336 (4.8)	311 (3.3)	332 (4.0)	25	56	1.458	0.6900

[a] Full width at half maximum. [b] Extinction coefficient $\times 10^{-4}$ at absorption maxima. [c] Absorption spectral maximum of aggregate relative to monomer. [d] $B = \epsilon_{312}/\epsilon_{332}$ for pure $_4A_4EPC$ vesicle; $B = \epsilon_{318}/\epsilon_{348}$ for pure vesicles of other three APL's. [e] $H = \epsilon_{312}/\epsilon_{332}$ for $_4A_4EPC$ highly diluted in DMPC vesicles; $H = \epsilon_{318}/\epsilon_{348}$ for other three APL's highly diluted in DMPC vesicles.

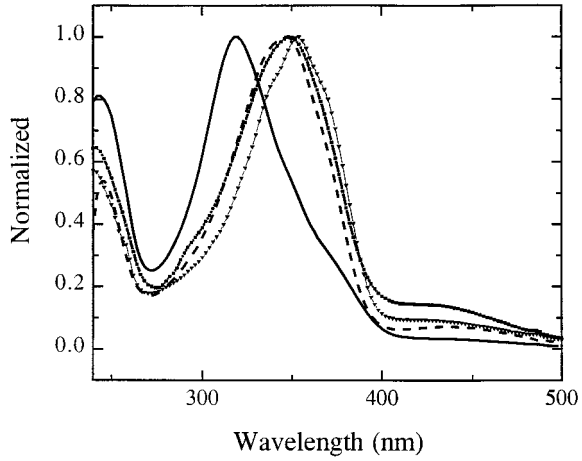

Figure 1. Absorption spectra of Ao_8EPC in water, chloroform, and DMPC; and Ao_8H in γ-CDN: (—) water, (- - -) DMPC, (-■-) γ-CDN, (-▼-) chloroform.

(Table 1). A comparison between the spectra of Ao_8EPC in water, chloroform, and water with excess saturated fatty acid phospholipid, dimyristoyl phosphatidyl choline (DMPC) co-solubilized, is shown in Figure 1. By analogy with results obtained for structurally similar amphiphiles such as the isoelectronic *trans*-stilbene derivatives[17] and tolans,[20] we assign the blue-shifted spectrum obtained in the aqueous dispersion of pure APL to an "H" aggregate[33] while the much less shifted spectrum in the APL:DMPC dispersions in water are attributed to a dimer. Evidently a polarity effect produces a red shift when the enviroment is changed from the hydrophobic bilayer of the vesicles to chloroform; in the case of dimer formation, the consequent blue shift associated with formation of an "H" dimer superimposed on the "solvent" red shift results in a net small blue shift. Similar spectral shifts are associated with the change in environment from monomer in an organic solvent to the dimeric complex in β- or γ-cyclodextrin in aqueous solutions. The azobenzophanes prepared in an earlier study which have a face-to-face relationship imposed in a rigid structure show a similar small blue shift in absorption.[34]

While the absorption spectra associated with the aggregate are similar for the different APL's, there are some significant differences (Figure 2). For example, the spectrum of Ao_8EPC in water is sharper and slightly more blue shifted than those of $_6Ao_2EPC$ and $Ao_{8,6}Ao_2EPC$. Possible reasons (see below) include either different aggregate sizes or a different packing within the aggregate. As we have observed earlier with the stilbene phospholipids[17] and other aggregating aromatics,[19,20] mixing of the "pure aggregate" solutions with aqueous solutions of excess saturated phospholipid such as DMPC results in an evolution of the aggregate spectrum to that associated with the dimer. The spectral changes observed upon mixing aqueous

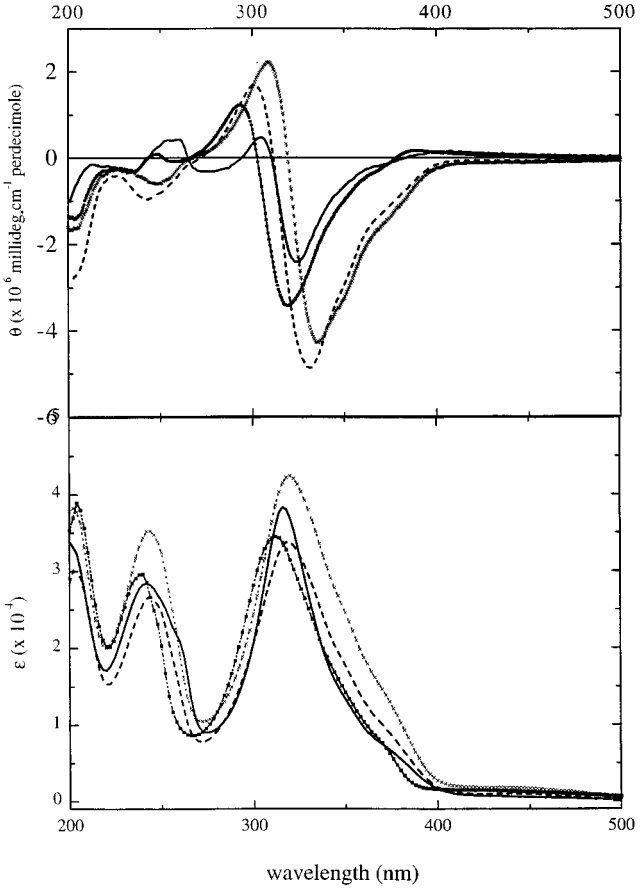

Figure 2. Absorption (upper) and ICD (lower) spectra of aqueous dispersions of pure APL's: (—) Ao_8EPC, (- - -) $_6Ao_2EPC$, (••×••) $Ao_{8,6}Ao_2EPC$, (••■••) $_4A_4EPC$.

APL's and aqueous DMPC (Figure 3, parts a and b show mixing with $_6Ao_2EPC$ and Ao_8EPC, respectively) illustrate some additional differences. For Ao_8EPC, it is clear from the mixing experiment that the band corresponding to the monomer "A" transition undergoes the characteristic blue shift associated with H aggregation while the "B" band undergoes a concurrent red shift during the aggregation (J shift).[33,35] A similar result is observed for $_4A_4EPC$. In contrast, for $_6Ao_2EPC$ and $Ao_{8,6}Ao_2EPC$, there appears almost no change in the "B" band from the H-aggregate solution of pure APL's to the dimer solution in DMPC vesicles. The H aggregation and J aggregation for A band and B band, respectively, of APL aggregates are also demonstrated by their strong excitonic ICD spectra (see below).

Physical Characterization of *trans*-Azobenzene Phospholipid Dispersions in Water. The aqueous "solutions" of pure APL's or APL-saturated phospholipid mixtures can be charac-

(33) (a) Kasha, M.; Rawls, H. R.; El-Bayoumi, M. *Pure Appl. Chem.* **1965,** *11*, 371. (b) Czikkely, V.; Försterling, H.; Kuhn, H. *Chem. Phys. Lett.* **1970,** *6*, 11. (c) Kasha, M. *Radiat. Res.* **1963**, *20*, 55. (c) Czikklely, V.; Försterling, H. D.; Kuhn, H. *Chem. Phys. Lett.* **1970**, *6*, 207.

(34) Rau, H.; Luddecke, E. *J. Am. Chem. Soc.* **1982**, *104*, 1616.

(35) The transition dipole associated with the A band lies along the long axis of the azobenzene while that for the B band is perpendicular to the long axis. The head-to-head alignment of the dipoles for the A band in the proposed trimeric structure corresponds to a head-to-tail arrangement of the dipoles of the B band, which should lead to a red shift in the latter transition.

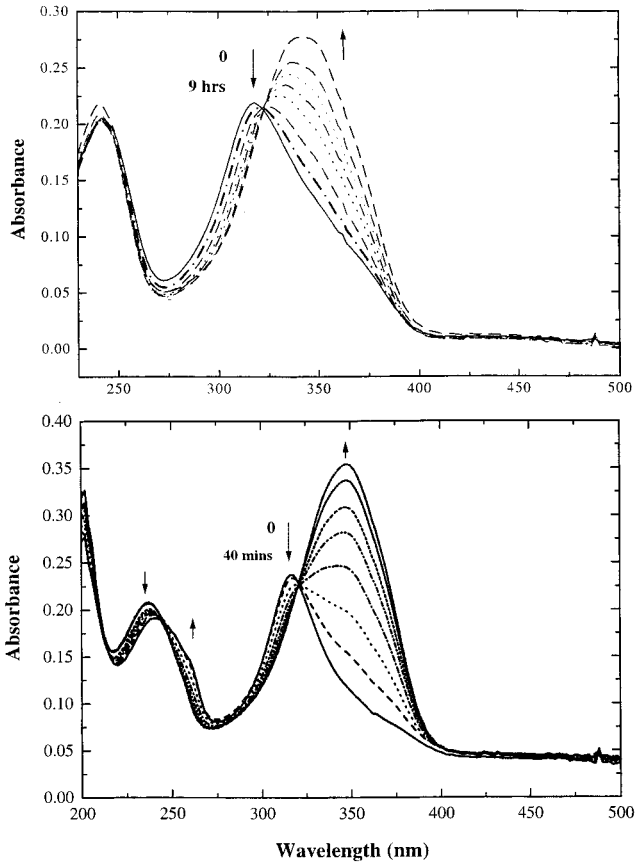

Figure 3. Dilution of aqueous dispersions of $_6Ao_2EPC$ (upper trace) and Ao_8EPC (lower trace) with DMPC as a function of time.

Table 2. DSC Data of Aqueous Dispersions of Pure APL's

	T, °C (major)	T_c, °C (minor)	Δ*H*, kcal/mol (major)
Ao_8EPC	74.5		11.1
$_6Ao_2EPC$	40.1	36.5	7.8
$Ao_{8,6}Ao_2EPC$	35.2	39.2	2.1
$_4A_4EPC$	45.5		6.2

terized by several different methods. In the present study we have used dynamic light scattering, microfiltration, differential scanning calorimetry (DSC), and cryo-transmission electron microscopy (Cryo-TEM). Microcalorimetry on aqueous dispersions of saturated phospholipids such as DPPC or DMPC which exist as bilayers (or even in multilamellar vesicles) shows evidence of phase transitions at 42 and 23 °C, respectively.[36] These are associated with chain melting or conversion through heating of a solid or gel form to a liquid crystalline state. For saturated phospholipids the phase-transition temperature is nearly independent of the precise state of the dispersion (unilamellar vesicle or multilamellar assembly) but highly dependent on chain length. Addition of sites of unsaturation either reduces the phase-transition temperature or eliminates the phase transition. The APL's are sufficiently soluble in water to observe phase transitions and measure the corresponding heat capacities; data in Table 2 and Figure 4 compare the phase-transition behaviors of four APL suspensions in water. The data obtained for $_4A_4EPC$ are consistent with the results reported in literature.[37] There is a clear trend among the three oxygenated APL's, which should all have about the same "hydrophobic" chain length; the phospholipid with the azobenzene farthest from the head group has a much higher T_c and a larger enthalpy for

(36) Kremer, J. M. H.; Kops-Werkhoven, M. M.; Pathmamanoharan, C.; Gijzeman, O. L. J.; Wiersema, P. H. *Biochim. Biophys. Acta* **1977**, *471*, 177.

(37) Morgan, C. G.; Thomas, E. W.; Sanhdu, S. S.; Yianni, Y. P.; Mitchell, A. C. *Biochim. Biophys. Acta* **1987**, 504.

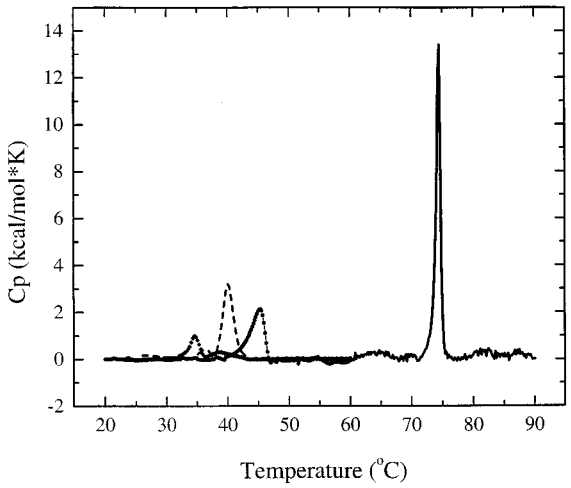

Figure 4. DSC of aqueous dispersions of pure APL's (scan rate = 60 °C/h): (—) Ao_8EPC, (- - -) $_6Ao_2EPC$, (··◆··) $Ao_{8,6}Ao_2EPC$, (··●··) $_4A_4$-EPC.

Table 3. Dynamic Light-Scattering Data for APL's (5×10^{-5} M)

	size (diameter), nm		intensity, $\times 10^{-5}$ M	
	trans	*cis*	*trans*	*cis*
Ao_8EPC	355	232	2.14	1.49
$_6Ao_2EPC$	86	82	0.91	0.92
$Ao_{8,6}Ao_2EPC$	71			
$_4A_4EPC$	92	102	1.32	1.45
DMPC and DPPC	10−20[a]			

[a] The size depends upon the preparation procedures; see ref 54.

the main transition than the APL with the azobenzene close to the head group while the "mixed" APL has an even lower T_c and a very small enthalpy of melting. $_4A_4EPC$, which has the azobenzene group in an intermediate position, has a T_c and enthalpy above that of $_6Ao_2EPC$ but below that of Ao_8EPC. As will be discussed later, the behavior observed is consistent with a somewhat different aggregate structure for the different APL's. For all four APL's it is found that there is little change in the absorption spectral maxima or band shape in aqueous dispersions over the temperature range 10−80 °C with the exception of a decrease in intensity. The persistence of photophysical properties over the range of temperatures where chain melting occurs suggests that the small domains or structural units which determine the photophysics persist and are relatively unperturbed by this phase-transition process. Similar but broader DSC peaks of DMPC and DPPC codispersed with APL's in water compared with pure DPPC or DMPC aqueous dispersions suggest the APL's are well solubilized in DPPC or DMPC bilayers.

The aqueous dispersions of the APL's scatter light, and dynamic light scattering can be used to estimate the size of the microparticles that are formed. Table 3 compares sizes (diameters, based on assumption of spherical particles) estimated by dynamic light scattering for the four *trans*-APL's and compares these estimated diameters with those of DMPC and DPPC. Values for the APL's following irradiation to form a *cis*-rich photostationary state are also listed in the Table 3. The particle size for Ao_8EPC was found to decrease while the other APL's showed little change on production of *cis* and no new distribution of particle sizes. The estimation of particle sizes on the order of or greater than 100 nm suggested that the APL assemblies might not pass through a 100 nm pore filter. In fact it was found that no *trans*-Ao_8EPC dispersions in water could be filtered through a 100 nm polycarbonate membrane. About half of the APL's in aqueous dispersions of *trans*-$_6Ao_2$-EPC, Ao_8, $_6Ao_2EPC$, and $_4A_4EPC$ could be extruded through a 100 nm polycarbonate membrane but no *trans*-APL could be

passed through a 20 nm polycarbonate membrane. This is consistent with sizes near 100 nm diameter for these APL's in water as indicated by the light-scattering data. An indication that the size of the APL particles in aqueous solution might be dramatically decreased by conversion of the *trans*-azobenzene to *cis* was found by filtration experiments following irradiation to form a *cis*-rich photostationary state. For Ao_8EPC it was found that a dispersion of *cis*-Ao_8EPC (as indicated by spectral changes following irradiation of *trans*) could be extruded almost completely through a 100 nm polycarbonate membrane but not through a 20 nm polycarbonate membrane.[38] The extruded solution of *cis* could be irradiated with a sun lamp (visible irradiation) or stored in the dark at room temperature for several hours, in either case resulting in conversion back to *trans;* the resulting dispersion failed to pass any *trans* upon extrusion through the 100 nm membrane (as indicated by lack of any absorption in the UV−visible following filtration). Similar experiments were performed with the other APL's; about half of *cis*-$_6Ao_2$EPC, $Ao_{8,6}Ao_2$EPC, and $_4A_4$EPC obtained by irradiation at 365 nm from the corresponding *trans* solutions could be extruded through 20 nm membranes. As with the Ao_8EPC, these samples could be reconverted to *trans* and the resulting solutions consisted of "particles" which could not pass through the 20 nm membrane. Initially, we thought that APL's dispersed in aqueous solutions might have formed spherical closed vesicle structures. They turned out not to be the case. We found that pure aqueous dispersions of APL's do not trap carboxyfluorescein (CF) as would be expected if closed bilayer vesicles are formed. A Cryo-TEM study of *trans*-Ao_8EPC aqueous dispersion (Figure 5a) shows very flat bilayer structures of extended or folded sheets which are apparently open structures and show little curvature while the Cryo-TEM image (Figure 5b) of a *cis*-Ao_8EPC sample prepared approximately a half hour after irradiation of *trans*-Ao_8EPC vesicles (a small percentage of the *cis*-APL's have thermally been converted back into *trans*-APL) exhibits both faceted, flat sheet structures and smaller spherical structures. A reasonable interpretation is that the aggregated chromophores of *trans*-Ao_8EPC resist the necessary curvature that would be required to form small unilamellar, spherical vesicles. The sizes (ranging from 100 to 300 nm in length and width for *trans*-Ao_8EPC and smaller structures for *cis*-Ao_8EPC rich sample) of microparticles from Cryo-TEM are consistent with the results from light-scattering and extrusion experiments. The TEM micrographs show no significant difference between the original *trans*-Ao_8EPC vesicles and *trans*-Ao_8EPC vesicles obtained from thermal and photoreisomerization of *cis*-Ao_8EPC solutions. *trans*-$_6Ao_2$EPC vesicles show totally different structures from the sheetlike structure of *trans*-Ao_8EPC vesicles. The Cryo-TEM of *trans*-$_6Ao_2$EPC vesicles shows fibrous structures (Figure 5c). Some fibers are as long as 1000 nm with diameters of a few nanometers.

Circular Dichroism (CD) Spectra of APL Vesicles. No induced circular dichroism (ICD) signals are detected for APL's in chloroform where the monomer is formed, except for $_6Ao_2$EPC which exhibits a weak biphasic CD spectrum with a positive Cotton effect (CE) at 480 nm and a negative CE at 340 nm. The two CE's are attributed to an oblique dimer of azobenzene which is also supported by its broad and slightly blue-shifted absorption spectrum.[39] The azobenzene H dimers of APL's highly diluted in DMPC or DPPC exhibit no CD signals while a small blue shift in the absorption spectra of the H dimers is observed. In contrast to the lack of or weak ICD for the monomer and dimer, strong ICD spectra (Figure 2) were observed for all pure APL vesicles. No linear dichroism signals have been detected for APL vesicles. Characteristic of the ICD spectra of Ao_8EPC and $_4A_4$EPC assemblies are triphasic ICD signals for the blue-shifted A band (H aggregation)[40] and biphasic ICD signals for red-shifted B band (J aggregation) while the ICD of $_6Ao_2$EPC and $Ao_{8,6}Ao_2$EPC vesicles have biphasic ICD signals from the H-aggregate A band and no significant signal for the B band. ICD data of APL aggregates are summarized in Table 4 (all vesicles were prepared by sonication followed by fast cooling to room temperature). The J aggregation of the B band of Ao_8EPC and $_4A_4$EPC vesicles was also observed in the absorption spectra which exhibit a small red shift relative to the monomer. The absorption peaks of the A bands and B bands of the aggregates lie at the wavelengths similar to those of the zero cross points of the excitonic ICD bands.[40] No CD signals have been observed for the n−π* transitions.

Although the blue-shifted absorption spectra of all four APL vesicles are independent of conditions used for preparation of the vesicles, their ICD spectra depend strongly upon the cooling rate of the sonicated aqueous solutions following the vesicle preparation. ICD spectra with reverse signs were obtained for $_6Ao_2$EPC and $Ao_{8,6}Ao_2$EPC vesicles for the fast and slow cooling procedures (Figure 6), while the ICD signals of $_4A_4$-EPC and Ao_8EPC vesicles are the same regardless of the cooling rate. The identical absorption spectra and reverse ICD spectra can be rationalized by the coexistence of two enantiomeric aggregates which have different energies originating from the chiral enviroment and their molecular structures. The measured apparent ICD spectra are summations of the ICD spectra of the populations of the two enantiomers in solution. For convenience, we label the aggregates with negative CE at long wavelengths and positive CE at short wavelengths of major A band as "R aggregates" and the aggregates with opposite ICD as "S aggregates". The R aggregates of $_6Ao_2$EPC and $Ao_{8,6}$-Ao_2EPC are converted into the S aggregates simply by heating, followed by slow cooling as indicated by the change in sign of the ICD spectra associated with the A band. The aggregation process is controlled by kinetics under the fast-cooling condition so that the kinetically favored enantiomer dominates. The slow conversion from the less stable enantiomer to the more stable below T_c increases dramatically at temperatures above T_c in the APL aqueous solutions. The R aggregates for Ao_8EPC and $_4A_4$-EPC are both kinetically and thermodynamically more stable while the R aggregates for $_6Ao_2$EPC and $Ao_{8,6}Ao_2$EPC are kinetically stable but thermodynamically less stable than the S aggregates.

Another interesting observation for APL vesicles is that the strong ICD signals disappear completely when the *trans*-APL vesicles are photoisomerized into *cis*-APL's by UV light. The *trans*-to-*cis* photoisomerization of the aggregates in APL bilayers is much slower (~30- and 130-fold slower for $_6Ao_2$-EPC and Ao_8EPC, respectively) than the azobenzene monomers of APL's in chloroform. Figure 7 shows absoprtion and ICD spectra of $_4A_4$EPC vesicles at different stages of isomerization from *trans* to *cis*. All the ICD spectra pass through the same

(38) In Table 3, the size of the aggregate from *cis*-Ao_8EPC is estimated from light scattering to be ~200 nm. Although, as a reviewer has pointed out, this may seem inconsistent with extrusion of *cis* through a 100 nm membrane, the light-scattering data are generally somewhat skewed toward larger sizes since big particles make larger contribution. Additionally, the measurements in Table 3 were made at times following irradiaition during which some thermal isomerization to *trans* had occurred.

(39) (a) Person, R. V.; Peterson, B. R.; Lighter, D. A. *J. Am. Chem. Soc*. **1994,** 116, 42. (b) Gargiulo, D.; Ikemoto, N.; Odingo, J.; Bozhkova, N.; Iwashita, T.; Berova, N.; Nakanishi, K. *J. Am. Chem. Soc*. **1994**, *116*, 3760. (c) Polonski, T. *J. Org. Chem*. **1993**, *58*, 255.

(40) (a) Ebrey, T. G.; Becker, B.; Mao, B.; Kilbride, P. *J. Mol. Biol*. **1977,** *112*, 377. (b) Wu, S.; El-Sayed, M. A. *Biophys. J*. **1991**, *60*, 190. (c) Cassim, J. Y. *Biophys. J*. **1992**, *63*, 1432.

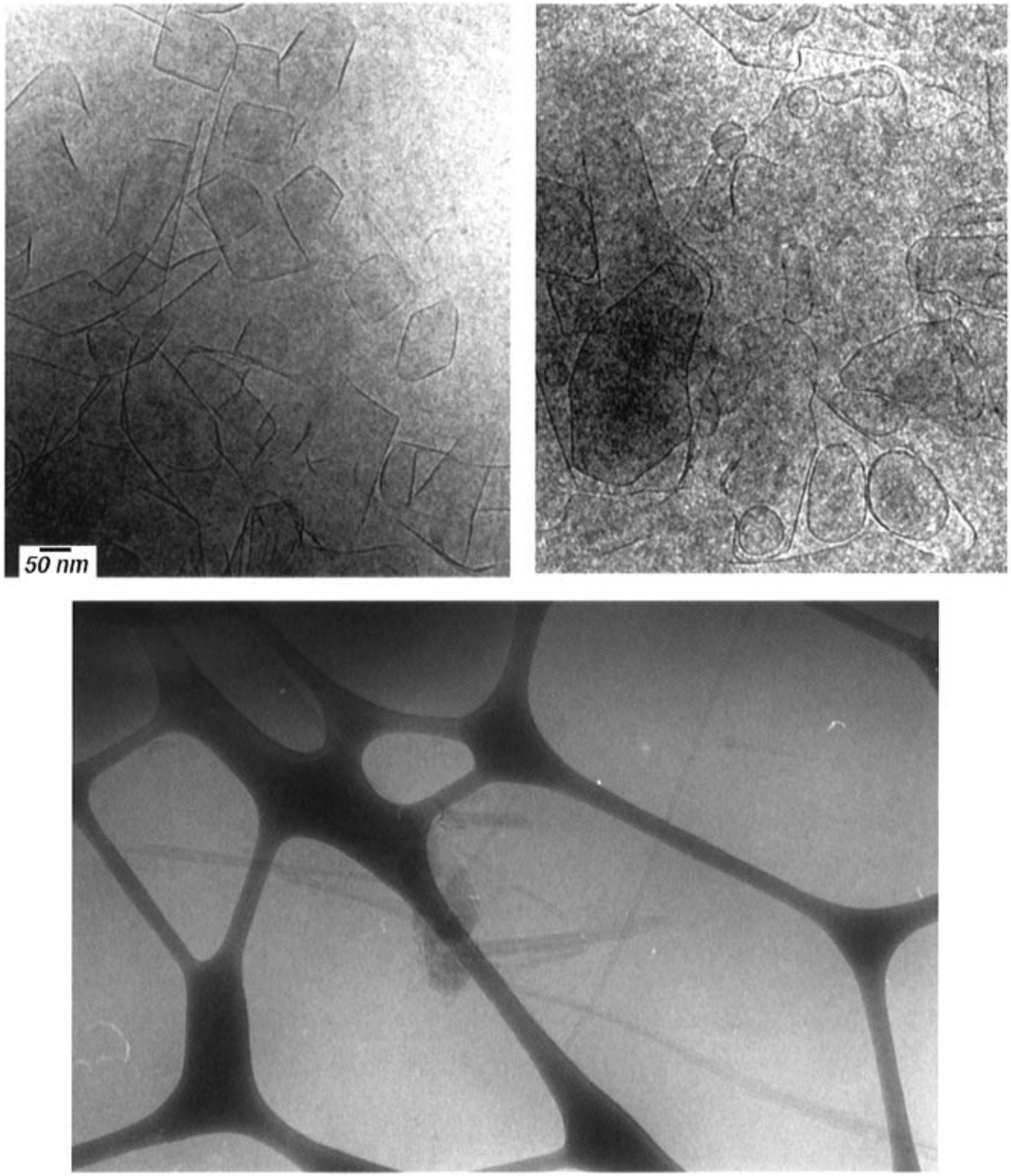

Figure 5. Cryo-TEM micrographs of aqueous dispersions of (a, upper left) *trans*-Ao_8EPC, (b, upper right) *cis*-Ao_8EPC, and (c, bottom) *trans*-$_6$-Ao_2EPC.

Table 4. ICD Data of Aqueous Dispersions of Pure APL's

	λ_{min}, nm	θ_{min},[a] $\times 10^{-5}$	λ_{max}, nm	θ_{max},[a] $\times 10^{-5}$	λ_t,[c] nm	θ_t,[a] $\times 10^{-5}$	$\lambda_{\theta=0}$, nm
Ao_8EPC	324 (277)[b]	−23.8 (3.1)	304 (256)	4.7 (4.4)	407	1.6	310 (256)
$_6Ao_2$EPC	331 (243)	−48.6 (9.4)	301	17.0			311
$Ao_{8,6}Ao_2$EPC	335 (246)	−42.3 (5.8)	309	22.0			319
$_4A_4$EPC	317 (258)	−34.0 (0.9)	293 (247)	12.0 (1.1)	387	1.6	302 (252)

[a] Molecular ellipticity (mdeg cm^2/dmol). [b] The data in parentheses correspond to B band. [c] Third CE for A band.

zero cross point and absorption spectra show two isosbestic points. The persistence of the ICD of the same aggregate even at relatively late stage of photoisomerization where most of *trans*-APL is transformed into *cis* is consistent with a small "unit" aggregate.[1] Other APL's show the same behavior. The blue-shifted absorption spectra of the aggregates of *trans*-APL's recover from the *cis*-rich solution by visible light irradiation. The ICD spectra of the newly formed *trans*-Ao_8EPC and *trans*-$_4A_4$EPC vesicles show little difference from the original *trans* solutions except in intensity which is higher for Ao_8EPC and

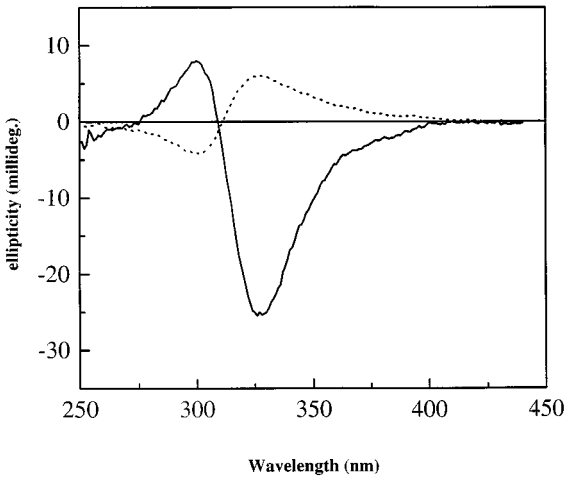

Figure 6. ICD spectra of aqueous dispersions of $_6Ao_2EPC$ prepared by different cooling procedures: (—) fast cooling, (···) slow cooling.

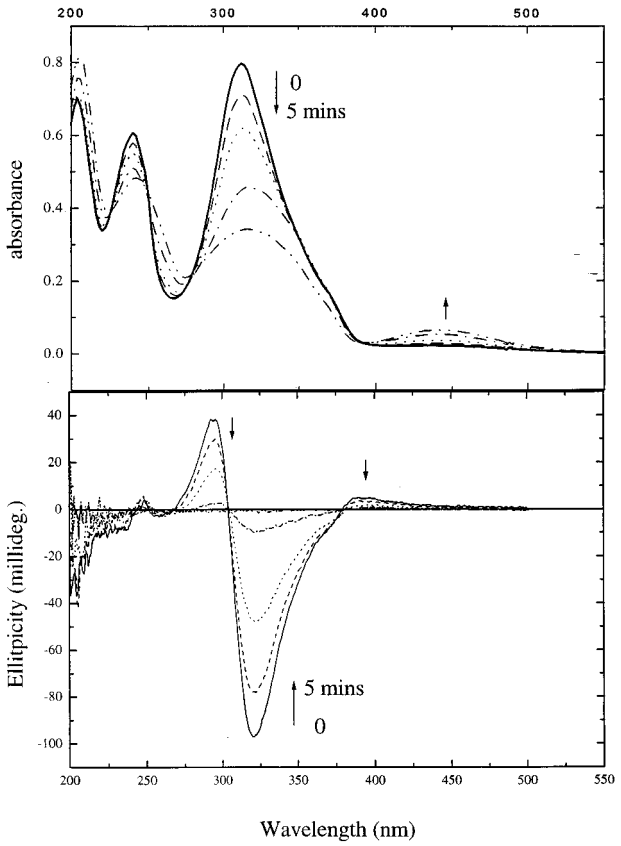

Figure 7. Absorption (upper) and ICD (lower) spectra of $_4A_4EPC$ aqueous dispersions as a function of irradiation time at 365 nm.

lower for $_4A_4EPC$ compared with original *trans* solutions. Interestingly, S aggregates dominate in the newly formed *trans*-$_6Ao_2EPC$ and *trans*-$Ao_{8,6}Ao_2EPC$ aqueous solutions (Figure 8). In these cases, the photoisomerization cycles of *trans*-APL aqueous dispersions result in the transformation of one enantiomer into the other.

APL's diluted with DMPC in moderate ratios show almost identical exciton ICD spectra to those of pure APL aggregates. This result supports the mixing experiments and equilibration between the aggregates and dimers which suggest no significant presence of other intermediate aggregates. Figure 9 shows the ICD spectra of $_6Ao_2EPC$ at different dilutions with DPPC and the intensity normalized ICD signals of APL in DPPC. All the spectra in different dilutions have a common zero cross point which indicates that the ICD signals are contributed from the same aggregate (the dimers are CD silent). The dependence of

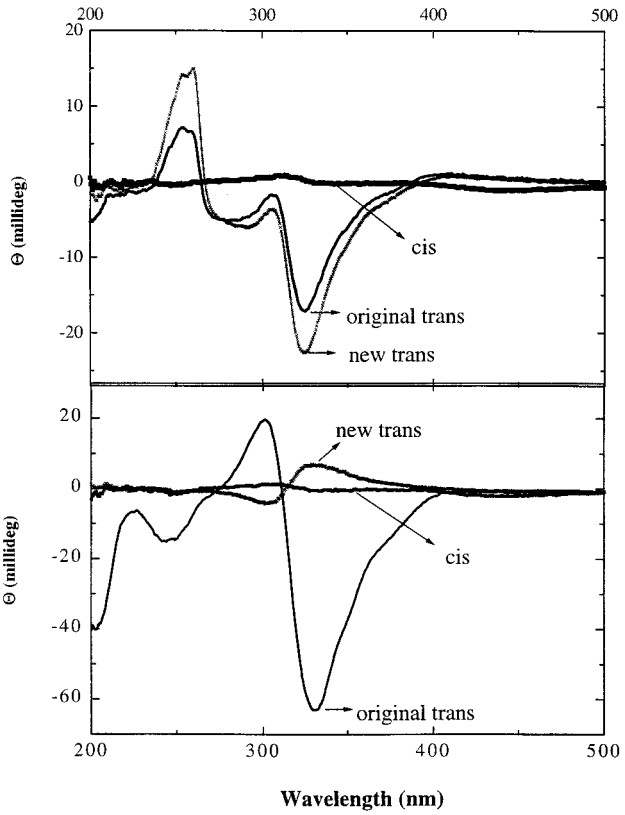

Figure 8. ICD spectra of Ao_8EPC (upper) and $_6Ao_2EPC$ (lower) aqueous dispersions through a reversible photoisomerizations cycle.

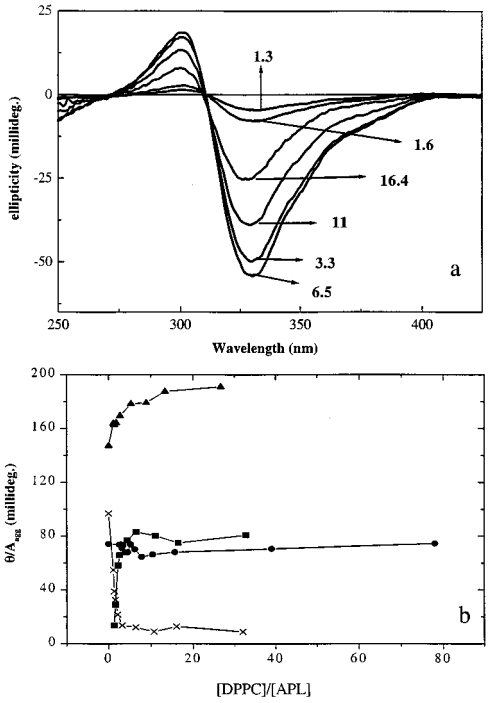

Figure 9. (a) ICD spectra of $_6Ao_2EPC$ in L-DPPC vesicles with various DPPC/$_6Ao_2EPC$ molar ratio. (b) The absorbance-normalized ICD intensity of the mixed vesicle solution vs the DPPC/APL molar ratio: (■) at 301 nm for $_6Ao_2EPC$, (▲) at 338 nm for $Ao_{8,6}Ao_2EPC$, (×) at 318 nm for $_4A_4EPC$, (●) at 327 nm for Ao_8EPC.

the intensity-normalized ICD signals on the dilution ratio clearly demonstrates the coexistence of both enantiomeric H aggregates which shift the equilibration between the two enantiomers due to the enviromental change of the matrix. The relative stability of the enantiomers depends upon both the positions of azobenzene in the fatty acid chains and the environment of the matrix. For $_6Ao_2EPC$ and $Ao_{8,6}Ao_2EPC$, the R-aggregate contribution

increases when the dilution becomes high while the R-aggregate contribution decreases for $_4A_4$EPC. In contrast, the relative contribution of both R and S aggregate does not change significantly for Ao_8EPC, as predicted by the relative large aggregates which experience little enviromental change by dilution of the matrix. The intensity-normalized ICD signal levels off when the dilution reaches a certain level beyond which further dilution does not cause significant environmental change experienced by the aggregates.

Estimation of Aggregate Sizes. Similar to stilbene-,[17] styrylthiophene-,[41] and tolan[20]-derivatized phospholipids, the evolution of absorption spectra of pure APL vesicles shows either one isosbestic point ($_6Ao_2$EPC, $Ao_{8,6}Ao_2$EPC, and $_4A_4$-EPC) or two (Ao_8EPC) when they are mixed with DPPC or DMPC vesicles at or above T_c (Figure 3). The result suggests that only two dominant species, an aggregate and a dimer, are involved in the process. The aggregate−dimer conversion can be accomplished either by changing the dilution ratio or the solution temperature. The absorption spectra of the mixture of APL and DMPC vesicles at different temperatures also display one isosbestic point. This indicates that the aggregates and dimers are in equilibrium with little contribution from other species so that the equilibration between dimers and aggregates can be expressed by eq 1. A modified Benisi−Hildebrand

$$\mathrm{Agg}_n\ (\mathrm{DMPC}) = n\mathrm{Dimer}\ (\mathrm{DMPC}) \tag{1}$$

approach[42] is used to formulate the equilibrium, and eq 7 is obtained in terms of the concentration and absorbance of aggregates and dimers in equilibrium solution with moderate dilution ratio. The plots according to eq 7 should be a straight line whose slopes allow determination of aggregate sizes n where n is the number of APL molecules for an aggregate. Equilibration between aggregate and dimer occurs in the DMPC matrix, which can be expressed by

$$K = [\mathrm{Di}]^n_{\mathrm{dmpc}}/[\mathrm{Agg}_n]_{\mathrm{dmpc}} \tag{2}$$

It should be noted that the concentrations used here refer to real concentrations in the DMPC microphase instead of the bulk aqueous solution concentration. For convenience, we replace the real concentrations in DMPC with concentrations in bulk solution by a simple conversion:

$$[\mathrm{Agg}_n]_{\mathrm{aq}} = [\mathrm{Agg}_n]_{\mathrm{dmpc}}\,(V_{\mathrm{dmpc}}/V_{\mathrm{aq}}) \tag{3}$$

$$[\mathrm{Di}]_{\mathrm{aq}} = [\mathrm{Di}]_{\mathrm{dmpc}}\,(V_{\mathrm{dmpc}}/V_{\mathrm{aq}}) \tag{4}$$

$$V_{\mathrm{dmpc}} = MV_{\mathrm{m}} \tag{5}$$

where V_{dmpc} is the volume of DMPC; V_{aq}, volume of aqueous solution; M, number of moles; and V_{m}, partial specific volume of DMPC which is considered to be constant.[43] Combination of eq 2−5 produces

$$K = [\mathrm{Di}]_{\mathrm{aq}}{}^n/\{[\mathrm{Agg}_n]_{\mathrm{aq}}[\mathrm{DMPC}]_{\mathrm{aq}}{}^{n-1}\,V_{\mathrm{m}}{}^{n-1}\} \tag{6}$$

Equation 7 can be obtained from eq 6, if [DMPC] is kept constant:

$$K = [\mathrm{Di}]_{\mathrm{aq}}{}^n/[\mathrm{Agg}_n]_{\mathrm{aq}}C$$

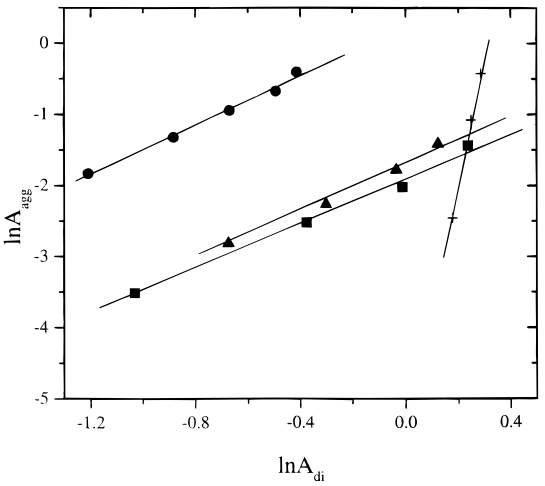

Figure 10. Benesi−Hildebrand plot of ln A_{agg} vs ln A_{di} of APL's in DMPC vesicles: (■) $_6Ao_2$EPC at 42 °C, (▲) $Ao_{8,6}Ao_2$EPC at 50 °C, (+) Ao_8EPC at 75 °C, (●) $_4A_4$EPC at 44 °C.

or

$$\ln[\mathrm{Agg}_n] = n\ln[\mathrm{Di}] + \mathrm{C}'$$

or

$$\ln A_{\mathrm{agg}} = n\ln A_{\mathrm{di}} + \mathrm{C}'' \tag{7}$$

Here, C, C', and C'' are constants and A_{agg} and A_{di} are absorbances of aggregates and dimers in equilibrium solution, respectively, which are easily obtained through eqs 8 and 9 where $A_t{}^x$ and $A_t{}^y$ are total absorbances at wavelengths of x and y, respectively; $B = \epsilon_{\mathrm{agg}}{}^x/\epsilon_{\mathrm{di}}{}^y$, the ratio of extinction coefficient at the peak wavelength (x) of aggregate, to that at the peak wavelength (y) of dimer or monomer, for the pure aggregate spectrum and $H = \epsilon_{\mathrm{di}}{}^x/\epsilon_{\mathrm{di}}{}^y$, the ratio of the extinction coeficient at the same two wavelengths for pure dimer or monomer absorption spectrum. The B and H for four APL's are listed in Table 1 along with the extinction coefficients of pure aggregates and dimers.

$$A_{\mathrm{agg}}{}^x = [H(A_t{}^y - A_t{}^x)]/[H/B - 1] \tag{8}$$

$$A_{\mathrm{di}}{}^y = [B(A_t{}^y - A_t{}^x)]/[B - H] \tag{9}$$

The plot of ln A_{agg} vs ln A_{di} show reasonable straight lines for all four APLs as shown in Figure 10. Aggregate sizes were measured to be 42 ($n = 21 \pm 4$), 3, 3, and 3 ($n = 1.7 \pm 0.2$)) in term of azobenzene chromophore for Ao_8EPC, $_6Ao_2$EPC, $Ao_{8,6}Ao_2$EPC, and $_4A_4$EPC, respectively. Surprisingly, the aggregate sizes of $_6Ao_2$EPC, $Ao_{8,6}Ao_2$EPC, and $_4A_4$EPC are much smaller than that of Ao_8EPC although their molecular structures are similar. The exceptionally large aggregate size for Ao_8EPC is consistent with its sharper and more blue-shifted absorption spectrum as well as its higher T_c.

The aggregate−dimer conversion for all APL's with the treatment of excess DMPC vesicles show pseudo-first-order kinetics for APL aggregates as observed for SPL's. Rate constants for the deaggregation processes of APL's are listed in Table 5 along with their equilibrium constants.

Monolayers and LB Films. Pure azobenzene derivatized fatty acids (AFH's) and APL's form monolayer films when spread from an evaporating chloroform solution over water at pH 6.8. The surface pressure area isotherms are shown in Figure 11 for Ao_8H and $_6Ao_2$H along with the reflectance spectra of the monolayers at the air−water interfaces and absorption spectra of LB films on quartz. The isotherms are relatively

(41) Song, X.; Whitten, D. G. Manuscript in preparation.
(42) Benesi, H. A.; Hildebrand, J. H. *J. Am. Chem. Soc*. **1949**, *71*, 2703.
(43) (a) Gennis, R. B. *Biomembranes, Molecular Structure and Function*; Springer-Verlarg: New York, 1989. (b) Fendler, J. H. *Membrane Mimetic Chemistry*; John Wiley & Sons: New York, 1982.

Table 5. Rate and Equilibrium Constants for Eq 1 for APL's at Different Temperatures

compounds	T (°C)	K^a	k (min^{-1})^b
$_4A_4$EPC	40	0.26	
	45		1.0×10^{-2}
Ao_8EPC	75	4.6×10^{-32}	
	70		1.1×10^{-1}
$_6Ao_2$EPC	50	1.5	
	45		2.0×10^{-3}
$Ao_{8,6}Ao_2$EPC	50	2.4	
	65		6.1×10^{-2}

[a] K is the equilibrium constants for eq 1; units depend upon n. [b] k is the pseudo-first-order rate constant for aggregate dissociation.

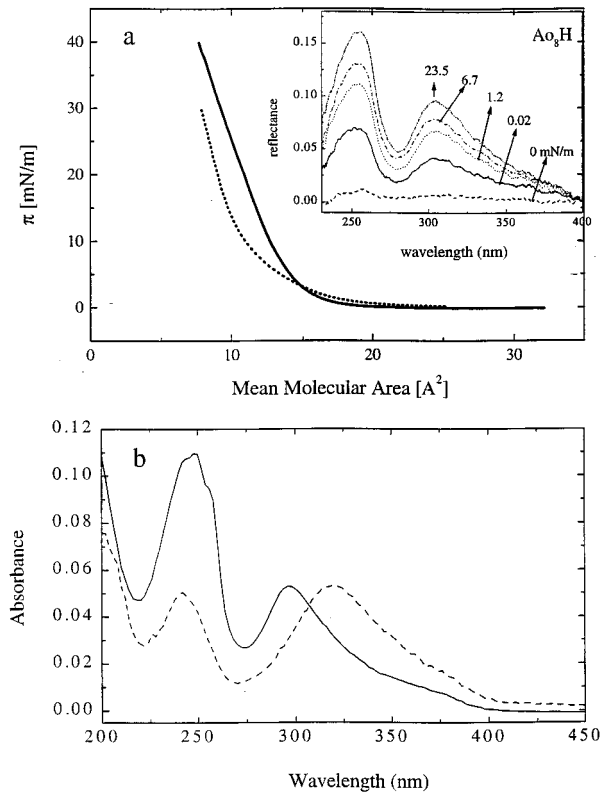

Figure 11. (a) Surface pressure area isotherms of AFH's monolayers. (Inset) Reflectance spectra of Ao_8H monolayer at different pressures. (b) Absorption spectra of AFH monolayers on quartz: (—) Ao_8H, (···) $_6Ao_2H$.

broad compared with those of fatty acids like arachidic acid. The molecular area from the isotherm is siginifcantly smaller than expected, probably due to some solubility of AFH's in water. The films at the air−water interface show almost identical reflectance spectra at different pressures with a dominant transition at 318 nm. The reflectance of the film is significantly blue shifted relative to monomer absportion spectra of AFH's and APL's in organic solvents such as chloroform and is quite similar to the blue-shifted absorption spectra obtained for APL vesicles or for LB film of Ao_8EPC on quartz. It is noteworthy that the blue-shifted spectrum is observed even at very low surface pressure (0.02 mN/m) where little "forced" packing of the chromophores is anticipated. The insensitivity of the reflectance spectra to the surface pressure suggests that the aggregate is a result of strong interaction between the azobenzene units prior to compression rather than formation of a forced assembly as a consequence of the compression and organization of the monolayer.[21]

The compressed monolayers of AFH's at the air−water interfaces can be readily transferred to solid supports such as quartz to form LB films. The LB film of $_6Ao_2H$ on quartz gives a blue-shifted absorption transition at 318 nm for A band similar to that observed in APL vesicles and the monolayer of Ao_8H at the air−water interfaces while the absorption A band of the LB film of Ao_8H is further blue shifted to 295 nm. The intensity for the A and B bands of the LB film of $_6Ao_2H$ are comparable. In contrast, the intensity of the B band is almost twice as high as A band of the LB film of Ao_8H. These different blue shifts of the aggregates for AFH LB films were also observed by other groups and can be rationalized by the different orientation of azobenzenes and aggregate sizes. In the LB films of Ao_8H, the aggregate is large and the major transition dipole moments of A band in the aggregate may be more perpendicularly oriented to the surface of the quartz than for the LB films of $_6Ao_2H$. The transition dipole moments of the B band in the LB film of Ao_8H should be perpendicular to the transition dipole of A band and nearly parallel to the plane of the quartz so that the strong interaction between the dipole and light coming from the perpendicular direction gives a strong absorption.

Photoregulatable CF Release From Vesicles. Much attention has been devoted to the potential of vesicles as a drug delivery vehicle,[44] mainly due to the compatibility of natural phospholpid vesicles with cell membranes, minimal toxicity, and easy control of drug release from vesicles by many techniques[22−24] such as hyperthermia,[45] pH-sensitive polymer surfactants,[46] and photochemistry. As a drug delivery system, it is very important that the release of drugs can be controlled easily and the vehicle must produce minimal side effects. Several studies have focused on photochemical perturbation of vesicle bilayers[22−24] which, to some extent, can promote the release of water soluble reagents. Here we have investigated photoisomerization of APL's to control the reagent release from vesicles as a function of the phospholipid structure, vesicle composition and aggregation state of the APL's. In this study, carboxyfluorescein (CF) was used as a fluorescence indicator to monitor change in pemeability of the vesicles.[29] The fluorescence intensity of CF in aqueous solution at very low concentration is proportional to [CF] while it fluoresces weakly due to self-quenching at high concentration (>100 mmol). Vesicles with high concentration of CF inside and free of CF outside can be prepared by gel filtration; the weak fluorescence of CF will increase due to its dilution if any leakage of CF occurs from the inside of vesicles to the bulk solution on the outside. Thus leakage of the CF from the vesicles is easily followed by monitoring the CF fluorescence. In these studies, 0.1 M CF aqueous solutions were used and ∼2000 CF molecules are estimated entrapped in one vesicle of an average size[47,48] (based on the assumption of 25 nm in diameter and 5 nm in thickness of the bilayer, see Cryo-TEM study below).

As expected from the open, flat, sheetlike structures observed for Cryo-TEM study of pure APL aqueous dispersions, pure APL vesicles do not entrap any CF. On the other hand, the vesicles formed from mixtures of APL or AFH and DPPC, where the azobenzene may exist as aggregates or dimer or monomer, entrap CF without significant leakage for extended periods of time (one week, for example) at room temperature or at 4 °C. The leakage of CF from the inside to the ouside of vesicles can be controlled by photoisomerization of azobenzene aggregates or other photoreactive chromophore-derivatized

(44) (a) Philippot, J. R.; Schuber, F. *Liposomes as Tools in Basic Research and Industry*; CRC Press: Ann Arbor, 1995. (b) Garber, B. P.; Schnur, J. M.; Chapman, D. *Biotechnological Application of Lipid Microstructures*; Plenum Press: New York, 1988.

(45) Yatvin, M. B.; Weinstein, J. N.; Dennis, H. W.; Blumenthal, R. *Science* **1978**, *202*, 1290.

(46) Thomas, T. L.; Tirrell, D. *Acc. Chem. Res.* **1992**, *25*, 336.

(47) Cullis, P. R.; Hope, M. J. In *Biochemistry of Lipids and Membranes*; Vance, D. E., Vance, J. E., Eds.; Benjamin/Cummings: Menlo Park, CA, 1985; pp 25−72.

(48) Humphry-Baker, R.; Thompson, D. H.; Lei, Y.; Hope, M.; Hurst, J. K. *Langmuir* **1991**, *7*, 2592.

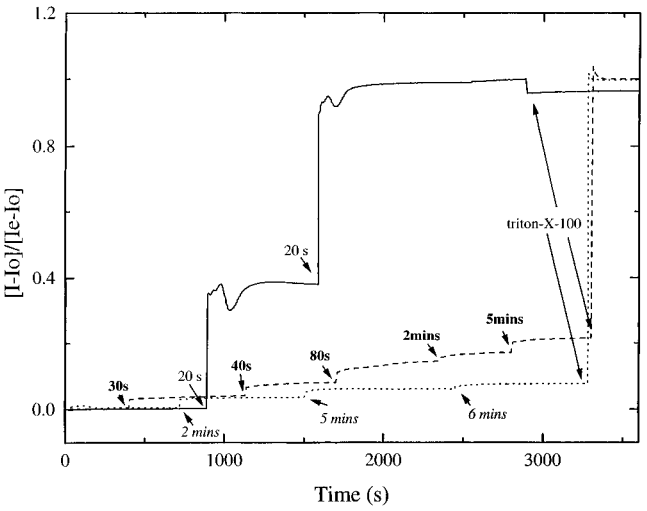

Figure 12. Fractional change in fluorescence intensity of trapped CF in vesicles uupon irradiation as a function of time. (I_o, I_e, and I) Initial intensity, final intensity after addition of 5% Triton-X-100 aqueous solution (0.05 mL), and intensity at any time, respectively: (---) [DPPC]/[$_6$Ao$_2$EPC] = 20, (···) [DPPC]/[Ao$_8$H] = 5, (—) [DPPC]/[$_6$Ao$_2$EPC] = 10.

surfactants. Figure 12 compares the fluorescence profiles of CF release upon irradiation at 365 nm for DPPC vesicles containing different percentages of $_6$Ao$_2$EPC and Ao$_8$H. When a 1:10 mixture of $_6$Ao$_2$EPC/DPPC (under conditions where ~30% of the APL is aggregated) is prepared with trapped CF, irradiation of the vesicles with 365 nm light for only a short time (40 s) results in total release of the CF concurrent with *trans*−*cis* isomerization of the azobenzene.[49] By controlling the length and power of irradiation, partial or total release of CF can be achieved. As a standard, total release can be achieved by addition of Triton-X-100.[29] In contrast, when vesicles containing mostly dimeric azobenzene (a 1:20 mixture of $_6$Ao$_2$-EPC/DPPC with similar optical density, where less than 10% APL is aggregated) or monomer (a 1:5 mixture of Ao$_8$H/DPPC where only monomer is expected) are irradiated, there is only a small amount of leakage in each case, even when most of the *trans*-azobenzene has been isomerized to *cis*. Irradiation with 365 nm light has almost no effect (as anticipated) upon the release of CF from pure DPPC vesicles. The results indicate that photoisomerization of the aggregates of the APL's is much more effective in promoting reagent release than an isolated photoisomerization process in a nonaggregated azobenzene or isolated dimer. Ao$_8$,$_6$Ao$_2$EPC and $_4$A$_4$EPC exhibit behavior similar to $_6$Ao$_2$EPC. Consistent with the high tendency for aggregation and larger H-aggregate size, a much lower percentage (less than 2%) of Ao$_8$EPC in DPPC is required to promote total CF release through photoisomerization.

An interesting feature of CF release induced by the photoisomerization of the aggregates of APL's is that very rapid release occurs only for the period of irradiation and the release drops immediately after irradiation stops for all the cases. A similar release pattern was observed for the interaction between DPPC vesicles and Triton-X-100 micelles.[29] This suggests that the release of CF is due to the complete disruption of vesicle structure. The formation of defects produced by the isomerization of Ao$_8$H monomer does not seem to promote any leakage of CF. The small amount of release in DPPC/APL's systems with relative high ratio (for example, [DPPC]/[APL] = 20) is also caused by disruption of vesicles due to the *trans*−*cis* isomerization of small number of aggregates. This disruption mechanism is also supported by Cryo-TEM studies. Aqueous solution of DPPC/$_6$Ao$_2$EPC (10/1) showed spherical vesicle structures which are similar to that of pure DPPC vesicles, The solutions obtained immediately after irradiation at 365nm showed many needle-like structures at the expense of spherical vesicles (Figure 13).

To clarify the effect of vesicle structure on the release pathway induced by photoisomerization of APL aggregates, we studied a series of vesicles containing different ratios of 1-palmitoyl-2-oleoyl-sn-glycero-3-phosphocholine/cholesterol (POPC/chol). The compactness of POPC vesicles (T_c = −5 °C) is easily tuned by incorporating cholesterol into vesicles. The vesicles made from POPC and POPC/chol exist in the fluid phase at room temperature. The compactness of the mixed fluid membrane, in general, tends to increase with increasing mole fraction of cholesterol.[29] In these studies, vesicle systems used were made from pure POPC, POPC/chol = 10/10, and pure DPPC with 10/1 molar ratio of lipids/$_6$Ao$_2$EPC, which are in increasing order of compactness. No significant leakage can be detected at room temperature without irradiation for all three systems. Figure 14 compares fluorescence intensity profiles of CF upon irradiation for these samples. After irradiation at 365 nm for short times (1 min) which converts *trans* completely into *cis*, for the DPPC/APL vesicles in the low temperature or solid phase, 100% release of CF is obtained. For POPC/chol = 10/10 in which the compactness of lipids is greater than POPC but less than for DPPC, ~30% CF is released by a "rupture" pathway and 70% by a slower leakage pathway. For the POPC vesicle, which is in fluid phase, a slow leakage pathway through which CF is released dominates to nearly 100%. Apparently the fluid state of vesicle favors a slow leakage pathway and the solid or gel phase favors the rupture process. A reasonable explanation is that for stiff DPPC vesicles, the integrity of the vesicle is lost on irradiation and the gel-phase lipids are not flexible enough to permit rapid healing. In contrast, we suspect, for POPC vesicles, release is through small defects caused by formation of *cis*-APL but that the vesicle structure remains intact. These results demonstrate clearly that permeability of vesicles can be tuned by choosing suitable lipid hosts and by modulating external conditions such as temperature and irradiation. The two different mechanisms are nicely supported by Cryo-TEM microscopy as shown in Figure 13. For DPPC/APL dispersions, all the spherical vesicle structures are converted into needle-like structures upon photoisomerization while no observable structural change occurs for POPC vesicles. In contrast, both needle-like and spherical vesicle structutres are observed for POPC/chol after irradiation.

Aggregate Structures and Possible Origins of Stablization for Aggregates. As has been done previously for monolayers of stilbene,[17c] styrylthiophene fatty acids,[41] and squaraine derivatives,[19] Monte Carlo cooling methods were applied to determine the apparent global and nearby local minimum structures of monolayer clusters of AFH's. The detailed procedures for the simulation have been reported elsewhere.[50] The apparent global minimum and several nearby lying local minima were found and the results are listed in Table 6 along with some calculated parameters and experimental data. Exciton shift spectra of the simulated structures were computed using the extended dipole-extended dipole method of Kuhn and coworkers.[51] For this computation, a transition moment of 6.09 D was estimated from the oscillator strength of the azobenzene monomer in solution at 348 nm, and the classical dipole length

(49) No attempt has been made to determine a quantitative (e.g., quantum yield) relationship between absorbed light intensity and CF release.

(50) (a) Chen, H.; Law, K. Y.; Perlstein, J.; Whitten, D. G. *J. Am. Chem. Soc*. **1995**, *117*, 7257. (b) Perlstein, J. *J. Am. Chem. Soc*. **1994**, *116*, 455. (c) Perlstein, J. *J. Am. Chem. Soc*. **1994**, *116*, 11420.

(51) (a) Czikkely, V.; Försterling, H.; Kuhn, H. *Chem. Phys. Lett*. **1970**, *6*, 11. (b) Kuhn, H.; Möbius, D.; Bücher, H. *Techniques of Chemistry*; Weissberger, A., Rositer, B. W.; Eds.; Wiley: New York, 1973; Part B, Vol. 1.

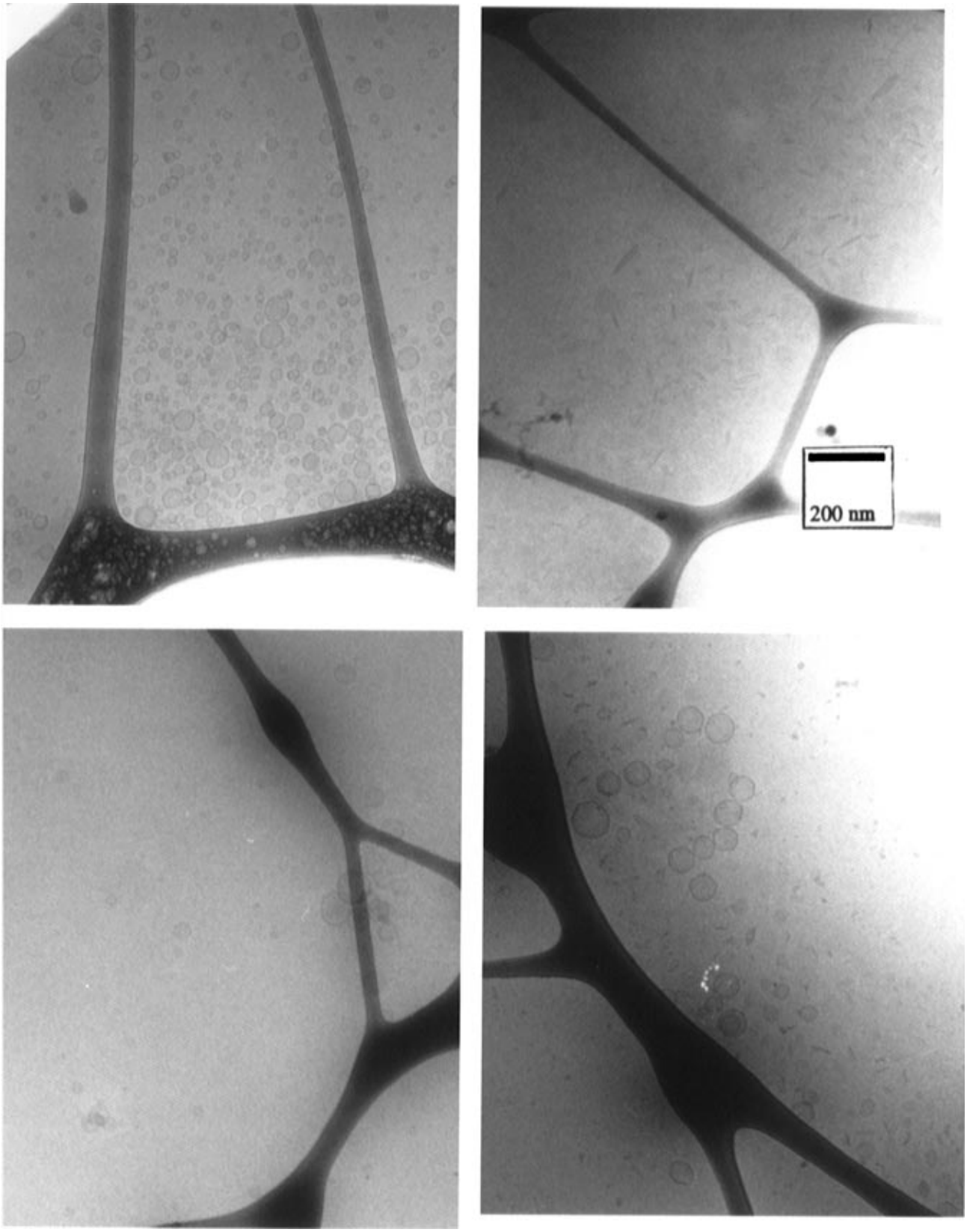

Figure 13. Cryo-TEM micrographs: mixed DPPC/*trans*-$_6$Ao$_2$EPC (10/1) vesicles before (a, upper left) and after (b, upper right) irradiation which results in a total release of CF, and mixed POPC/chol/*trans*-$_6$Ao$_2$EPC (10/10/1) vesicles before (c, lower left) and after (d, lower right) irradiation which results in partial release of trapped CF.

was estimated from the carbon−carbon end−end distance for *trans*-azobenzene of 10.43 Å. The dielectric constant was assumed to be 2.5. The computation was found to converge for a layer structure of 14 × 14 unit cells. The glide layers show a Davydov splitting whose oscillator strength ratio was estimated from the resultant vector sum and difference of the classical transition moments. The lowest energy structure which shows closest agreement with the experimental result, is the first local minimum glide layer for Ao$_8$H. An overhead view of this glide layer (showing only azobenzenes) is shown in Figure 15 along with schematic representation of a trimer isolated from the first local minimum structure of Ao$_8$H monolayer. Although we have not been able to calculate the possible structures of APL bilayers, similarities in their absorp-

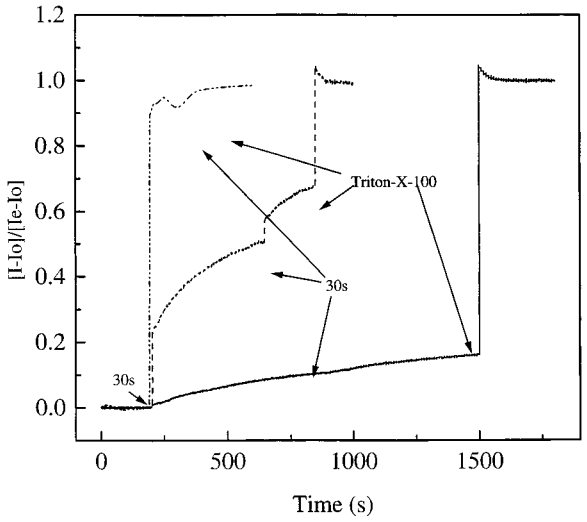

Figure 14. Fractional change in fluorescence intensity of trapped CF in vesicles upon irradiation versus time. I_o, I_e, and I have identical meanings as in Figure 12: (—) [POPC]/$_6$Ao$_2$EPC] = 10/1, (- - -) [POPC]/[chol]/$_6$Ao$_2$EPC] = 10/10/1, (- -—) [DPPC]/[$_6$Ao$_2$EPC] = 10.

Table 6. Predicted Unit Cell, Surface Area/Molecule, and Spectral Shifts for Ao$_8$H Monolayer

AFH	layer type	a^a	b^a	γ^a	surface area^b	$\lambda_1{}^c$	$\lambda_2{}^c$	ratio^d	energy^e
Ao$_8$H	glide	4.70	10.89	90.0	25.59	331	349	0.01	
	glide	5.81	7.51	90.0	21.82	320	352	0.01	0.84
	glide	4.98	9.47	90.0	23.58	328	350	0.01	1.09
	glide	4.68	9.18	90.0	21.48	320	351	0.00	1.23
	exptl				*f*	318	*g*	*g*	

^{a} Unit cell dimensions in Å; angle in deg. ^{b} Surface area/molecule in Å^2. ^{c} Exciton spectra peaks in nanometers; λ_1 and λ_2 for the glide layer as a result of Davydov splitting. ^{d} Computed ratio of the oscillator strength $f(\lambda_2)/f(\lambda_1)$ for the Davydov splitting. ^{e} Energy above the apparent global minimum in kcal. ^{f} Accurate surface area cannot be obtained due to its relatively high solubility in water. ^{g} The peak is too small to be identified.

tion spectra suggest that they may have similar aggregate structures. On the basis of the measured aggregation numbers and chiral nature, asymmetric trimers of an extended glide layer are proposed as the smallest aggregate unit while the extended structure should consist of a mosaic of trimers.[52] This arrangement is very similar to that concluded as the most likely structure for spectrally blue-shifted aggregates observed for other aromatic chromophores such as *trans*-stilbene, tolan, and squaraine derivatives, and it may well be a general supramolecular structure from which larger crystallites or aggregates may be constructed.[53] Excitonic interaction for the three degenerate transition dipole moments within the nonsymmetric trimeric "unit" aggregates produces excitonic states with three nondegenerate energy levels.[33,38] The relative intensities of the three optical transitions will depend on the specific details of the structural geometry.[38] For Ao$_8$EPC and $_4$A$_4$EPC aggregates, we observed two strong and one weak bands, whereas for $_6$Ao$_2$EPC and Ao$_{8,6}$Ao$_2$EPC aggregates we observed only two strong bands. The difference in ICD spectra of Ao$_8$EPC and $_4$A$_4$EPC aggregates compared to those for $_6$Ao$_2$EPC and Ao$_{8,6}$Ao$_2$EPC aggregates indicates some perturbation and distortion in the aggregate structures caused by the different position of azobenzene chromophores in the fatty acid chains.

Ao$_{8,6}$Ao$_2$EPC was originally designed to favor J-aggregate formation because its two azobenzenes have six offset methylene groups which presumably should favor the slipped stack arrangement. Surprisingly, similar H aggregates are formed, which implies that the H aggregates may be more stable than the corresponding J aggregates as was also observed for the mixture of squaraine derivatives at air−water interfaces. In those studies,[21] the J aggregates formed during the first compression eventually completely transformed into H aggregates after a few compression−decompression cycles. Many factors such as the spontaneous formation of aggregates in the AFH monolayers at the air−water interface without compression and the persistence of the aggregates in the APL solutions moderately diluted in saturated phospholipid vesicles suggest the relative stability of the aggregates. The glide arrangement of the azobenzenes in the aggregates is reasonable in terms of the likely maximization of the weakly $\sigma-\pi$ attractive interaction and minimization of $\pi-\pi$ repulsion[54] between stilbene chromophores. Such maximization of $\sigma-\pi$ attraction and minimization of $\pi-\pi$ repulsion may help stablize the aggregates. Another interesting aspect about the small H aggregates of azobenzene is that the energetically favored enantiomer for APL's with chromophores far away from head groups have opposite chirality to the favored one for APL's with chromophores close to the head groups. The apparent ICD spectrum reflects only the enantiomer with excess population. Their relative stability for the two enantiomers of the aggregates are possibly determined by the chirality of head group, the position of chromophores, and environments in which they are formed.

Similar to the stilbene dimer,[17] the azobenzene dimer also does not exhibit significant shift in absorption while the trimer gives a large blue shift. It may be attributed to some additional interaction which is not possible for the dimer. Higher stability of the unit aggregates over the dimer for stilbene and squaraine also supports the possibility that other interaction (bonding) besides hydrophobic and nonpolar interactions is involved. For extended aggregates for some azobenzene fatty acids in LB films, the observed largest shift in absorption spectra of H aggregates is 53 nm. Several azobenzene fatty acids incorporated into LB films have been observed to have 30 nm shifts which is the same as in vesicles. This seems reasonable that, in the former case, the relatively extended aggregate is formed while, in the later case, a mosaic of small aggregates (trimer) is formed as in vesicle solutions.[55,56]

Summary

For all the amphiphilic azobenzene fatty acids and phospholipids investigated in the present study, it is clear that azobenzene may exist as several different species, depending upon its state and the medium in which it is dispersed. Most of the AFH's and APL's when dissolved in organic solvents are readily identified as monomer from their absorption spectra. The AFH's in β- and γ-cyclodextrins and APL's diluted in excess DPPC or DMPC as well as $_6$Ao$_2$EPC in organic solvents were

(52) We infer that the extended arrays (mosaics) are regular glide or herringbone structures, such as found in the simulation or in the crystals of amphiphilic stilbenes,[53] with similar intermolecular interaction to those in the trimer "unit aggregate". This, of course, does not explain the observation that the limiting spectral shifts appear, in most cases, with the formation of the unit aggregate. At present, we have no satisfactory explanation for this.

(53) Vaday, S.; Geiger, H. C.; Perlstein, J.; Whitten, D. G. *J. Phys. Chem.* **1997**, *101*, 321.

(54) (a) Arunan, E.; Gutowsky, H. S. *J. Chem. Phys.* **1993**, *98*, 4294. (b) Hall, D.; Williams, D. F. *Acta Crystallogr.* **1975**, *A31*, 56. (c) Schweitzer, B. A.; Kool, E. T. *J. Am. Chem. Soc.* **1995**, *117*, 1863. (d) Winnik, F. M. *Chem. Rev.* **1993**, *93*, 587. (e) Linse, P. *J. Am. Chem. Soc.* **1993**, *115*, 8793. (f) Hunter, C. A.; Saunders, J. K. M. *J. Am. Chem. Soc.* **1990**, *112*, 5525. (g) Jorgenson, W. L.; Severance, D. L. *J. Am. Chem. Soc.* **1990**, *112*, 4768. (h) Shi, X.; Bartell, L. S. *Phys. Chem.* **1988**, *92*, 5667. (i) Pawliszyn, J.; Szczesniak, M. M.; Scheiner, S. *J. Phys. Chem.* **1984**, *88*, 1726.

(55) Kawai, T.; Umemura, J.; Takenaka, T. *Langmuir.* **1989**, *5*, 1378.

(56) An alternative explanation is that the difference in absorption spectral shift is attributed to the different orientation of azobenzene chromophores in the aggregates.

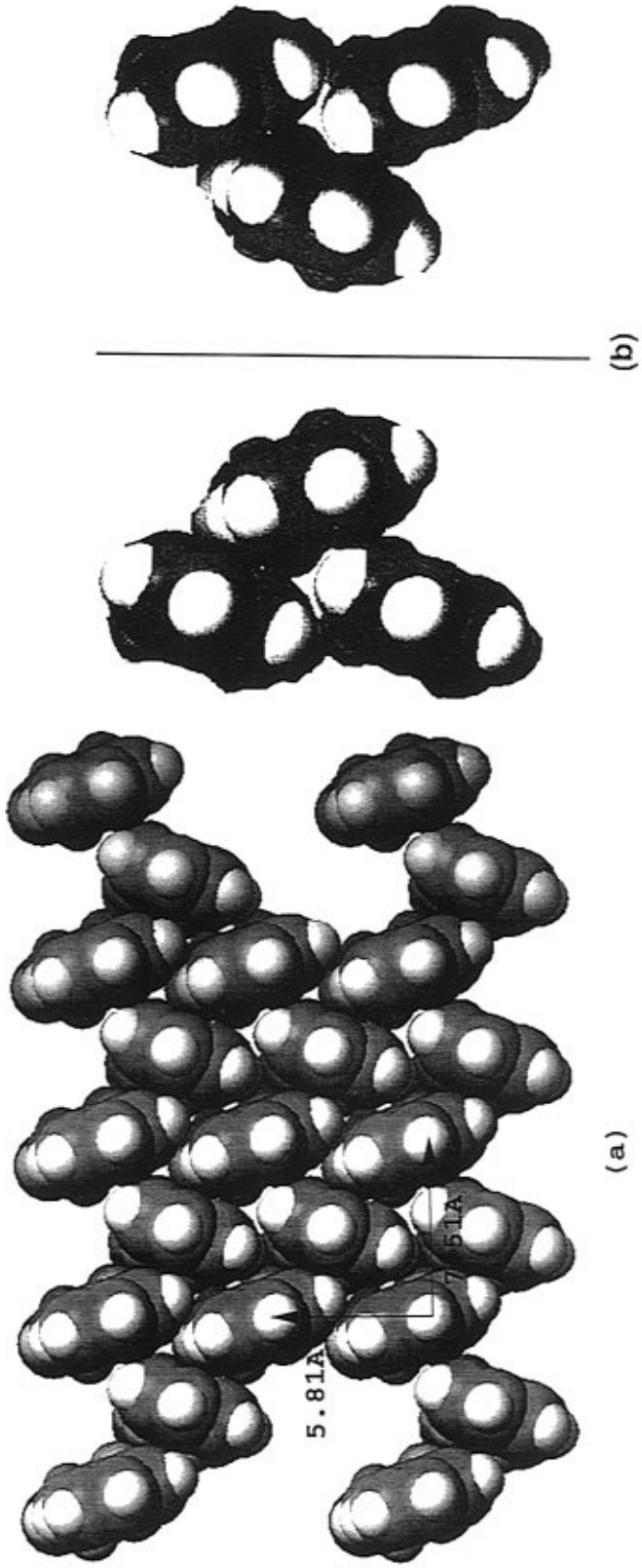

Figure 15. (a) Overhead view for the first local minimum of Ao_8H glide layer obtained from Monte Carlo simulation. Tilted 24.78° with respect to surface normal. The 7.51 Å *b* axis points to the right and the 5.81 Å *a* axis points to the top. (b) Two enantiomeric trimers isolated from the glide layer.

found to form azobenzene dimers based on their small blue shift in absorption similar to that of azobenzophanes and the weak biphasic ICD signals observed in some cases. From the studies of the monolayers, LB films of AFH's and bilayers of APL's in aqueous solutions, it is seen that the formation of similarly spectrally blue-shifted aggregates is a very general process as observed for other aromatics such stilbene and styrylthiophene as well as squaraine.[21,57] It is observed that the position of the azobenzene chromophore in the fatty acid chain of APL's plays important roles in controlling strength of the aggregation as demonstrated by the unusually large and well-organized aggregate and high T_c of Ao_8EPC. The clear tendency of azobenzene to form these aggregates reinforces the idea of a relatively high stability for the "unit" H aggregate. The proposed trimers for the unit aggregate are also supported by the unusual triphasic ICD of A bands for $_4A_4$EPC and Ao_8EPC vesicles.

Aggregation of chromophores results in some novel photophysical and photochemical properties such as the sharp, blue-shifted absortpion spectrum and the less efficient *trans*−*cis* photoisomerization compared with the isolated monomer. Photoisomerization of the azobenzene aggregates provides a very convenient way to enhance membrane permeability, which may have some potential applications as useful photoregulatable materials. We have also demonstrated the likely mechanistic pathways for the reagent release from vesicles through photoisomerization of azobenzene aggregates and modulation of the release mechanism by adjustment of the vesicle composition.

Acknowledgment. We are grateful to the U.S. National Science Foundation (Grant CHE-9521048) for support of this research.

JA971291N

(57) Chen, H.; Farahat, C. W.; Farahat, M. S.; Geiger, C. H.; Leinhos, U.; Liang, K.; Song, X.; Penner, T. L.; Ulman, A.; Perlstein, J.; Law, K. Y.; Whitten, D. G. *Mater. Res. Soc. Bull*: *Organic Thin Film* **1995**, *20*, 39.